Classification:
Major category: Biological Sciences
Minor Category: Neuroscience

Synthetic zinc finger repressors reduce mutant Huntingtin expression in the brain of R6/2 mice

Mireia Garriga-Canut[a,2], Carmen Agustín-Pavón[a,b,2], Frank Herrmann[a], Aurora Sánchez[c], Mara Dierssen[b], Cristina Fillat[d] and Mark Isalan[a,1]

Proceedings of the National Academy of Sciences of the United States of America, 109(45), 2012 DOI: 10.1073/pnas.1206506109

[a]EMBL/CRG Systems Biology Research Unit, and [b]Genes and Disease Programme, Centre for Genomic Regulation (CRG) and UPF, Dr. Aiguader 88, 08003 Barcelona, Spain.
[c]Servei de Bioquímica i Genètica Molecular, Hospital Clínic, 08028 Barcelona, Spain.
[d]Institut d'Investigacions Biomèdiques August Pi i Sunyer (IDIBAPS) and Centro de Investigación Biomédica en Red de Enfermedades Raras (CIBERER), Barcelona

[1]Corresponding author: Mark Isalan, EMBL/CRG Systems Biology Research Unit, Centre for Genomic Regulation (CRG) and UPF, Dr. Aiguader 88, 08003 Barcelona, Spain. Telephone number: +34 93 316 0158. Email: mark.isalan@crg.eu.
[2]These authors contributed equally to this work.

Abstract

Huntington's disease (HD) is a dominantly-inherited neurodegenerative disorder caused by expanded CAG repeats in the huntingtin (*HTT*) gene. Although several palliative treatments are available, there is currently no cure and patients generally die 10 to 15 years after diagnosis. Several promising approaches for HD-therapy are currently in development, including RNAi and antisense analogues. We developed a complementary strategy to test repression of mutant *HTT* with zinc finger proteins (ZFP) in an HD model. We tested a 'molecular tape measure' approach, using long artificial ZFP chains, designed to bind longer CAG repeats more strongly than shorter repeats. After optimisation, stable ZFP expression in a model HD cell line reduced chromosomal expression of the mutant gene at both the protein and mRNA level (95% and 78% reduction, respectively). This was achieved chromosomally in the context of endogenous mouse *HTT* genes, with variable CAG repeat-lengths. Shorter wild-type alleles, other genomic CAG-repeat genes, and neighbouring genes were unaffected. *In vivo*, striatal AAV viral delivery in R6/2 mice was efficient and revealed dose-dependent repression of mutant *HTT* in the brain (up to 60%). Furthermore, zinc finger repression was tested at several levels, resulting in protein aggregate reduction, reduced decline in rotarod performance, and alleviation of clasping in R6/2 mice, establishing a proof-of-principle for synthetic transcription factor repressors in the brain.

/body

Introduction

The pathological expansion of CAG repeats leads to extended polyglutamine (polyQ) tracts in mutated gene products (1). The resulting proteins are thought to aggregate and cause toxic gain-of-function diseases, including spinocerebellar ataxias, spinobulbar muscular atrophy and Huntington's disease (HD) (2, 3). HD neuropathology is associated with selective neuronal cell death, primarily of medium spiny neurons of the striatum and, to a lesser extent, cortical neurons, causing cognitive dysfunction and chorea (1, 4). Since the discovery, in 1993, that the huntingtin (*HTT*) gene caused HD (5), much attention has been focused on how the CAG-repeat number affects the pathology and progression of the disease; normally, the number of CAG repeats in the wild-type (wt) *HTT* gene ranges from 10 to 29 (median 18) (1, 4), whereas HD patients typically range from 36 to 121 (median 44) (1, 4). Because the age of onset of disease is correlated to CAG repeat number (1), reducing the polyQ 'load' on cells should be beneficial therapeutically.

Despite intense research, there is no way to stop or delay the progression of HD and current treatments merely treat symptoms (1, 4). However, a number of promising studies have aimed at improving cell survival of affected areas (reviewed in (6)). Unlike other neurological disorders, such as Alzheimer's and Parkinson's diseases, HD is monogenic (5). Therefore, therapeutic strategies need only target the expression of the causal gene, to reverse and treat the effects of the mutant protein. However, since wt HTT protein is widely expressed (7), is essential for early embryonic development (8) and is required for neuronal function and survival in the brain (9), it is important to specifically reduce the expression of the mutant protein, while leaving the expression of the wt protein as unaffected as possible.

Several approaches using synthetic nucleic acids that selectively target the mutant allele are currently being developed (reviewed in (10)). Recently, RNA interference (RNAi) was shown to reduce expression of mutant *HTT* (11-13). Although this technique could be very powerful, mutant-selective RNAi depends on targeting single nucleotide or deletion polymorphisms that differentiate between alleles, and these often differ from patient to patient. However, there is evidence that partial repression of wt *HTT* can be tolerated (14, 15), suggesting that generic approaches that repress both alleles should also be pursued. Peptide and locked nucleic acids (PNAs and LNAs) are generic and yet some promising partially-selective inhibition of expanded CAG repeats of the ataxin-3 and *HTT* genes has been reported (16, 17). Recently, there has even been sustained disease reversal using antisense oligonucleotides (18).

Also aiming to reduce the levels of mutant protein, a different approach was proposed by Bauer et al. who designed a polyglutamine-binding peptide, fused to heat shock cognate protein 70 binding motif, to direct degradation of mutant HTT via chaperone-mediated autophagy (19). Intrastriatal recombinant adeno-associated virus (rAAV) delivery of this fusion protein showed a strong therapeutic effect.

In this study, we examined the use of zinc finger proteins (ZFP) as a complementary approach to reduce the expression of mutant *HTT,* which could be used in tandem with any of the above approaches. Because zinc fingers can be readily re-engineered to bind different DNA sequences (20-29), including CAG-repeats (30), they could in

principle be used to target the *HTT* gene at a transcriptional level. Furthermore, zinc fingers can be easily concatenated into long chains, and different linker designs can alter the interaction kinetics substantially (31). This suggested to us that a systematic appraisal of different-length ZFP, with appropriate linker designs, might reveal an optimal configuration for repressing mutant *HTT*, while leaving the wt allele relatively unaffected.

We therefore designed a ZFP able to recognize and bind poly-5'-GC (A/T)-3', such that it would recognize both poly-CAG and its complementary DNA strand. The resulting ZFP chains (from 4- to 18-fingers) were able to repress target genes with longer CAG repeats preferentially, when compared to shorter repeats. This was carried out both in transient transfection reporter assays and with stable expression for 20 days, against full *HTT* chromosomal targets, in various model cell lines for HD. Ultimately, we tested the most effective ZFP *in vivo* in the R6/2 HD mouse model, using AAV for delivery, establishing a proof-of-principle for gene repression by synthetic zinc fingers in the brain.

Results

Designing long ZFP chains to bind expanded CAG repeats. Zinc fingers can be concatenated to make long multi-finger chains (31, 32) and, to date, no one has systematically explored the binding modes of different-length ZFP to long repetitive DNA tracts. We therefore used rational design to construct a zinc finger (ZFxHunt) that would bind 5'-GC (A/T)-3', such that poly-finger proteins would bind poly-GCA and poly-GCT (see Methods; Fig. 1). Both DNA strands were targeted to increase the avidity for low-copy chromosomal targets. For structural reasons, zinc finger chains with canonical linkers lose their register with cognate DNA after 3 fingers. Therefore, extra -Gly (31) or 29-residue linkers were added after every 2- and 6-fingers, respectively (full sequences given in SI). In this way, different numbers of fingers could be tested for length-dependent discrimination.

First, zinc finger chains containing either 4, 6 or 12 ZFxHunt domains were constructed and tested in gel shift assays, for binding to double-stranded CAG probes; longer ZFPs gave more complete binding (Fig. 1B). Intriguingly, distinct bound

complexes were observed, indicating that the ZFPs found single thermodynamic equilibria and were not trapped by kinetic intermediates. Highly-repetitive zinc fingers and DNA might have been expected to form contiguous partial binding events, which would have resulted in broad smears in gel shifts; this is not the case. Nonetheless, the 12-finger ZFP did give a lower, secondary shift, presumably caused by a 6-finger degradation by-product (zinc fingers can be unstable in linker regions (33)). To our knowledge, these 12-finger (and subsequently 18-finger) domains are the longest functional artificial ZFP chains ever built.

To test whether ZFxHunt proteins are able to bind both strands of a CAG DNA probe, ZF6xHunt was assayed by gel shift, and was shown to bind equally to both a CAG repetitive probe, $(GCA)_{x6}$, and to an alternate CAG-CTG probe, $(GCA\text{-}GCT)_{x3}$ (Fig. 1C). Furthermore, when compared to mutated sequences, ZF6xHunt showed specificity for $(CAG)_{x7}$ (Fig. 1D). In summary, we built multi-finger ZFP able to bind poly 5'-GC (A/T)-3' DNA probes specifically and efficiently *in vitro*.

Repression of polyQ reporter genes. Our starting hypothesis was that zinc finger proteins could preferentially bind longer CAG repeats through a mass action mechanism. Longer CAG repeats contain more target sites, and so should be bound and repressed more at any given ZFP concentration. Similarly, longer ZFP chains should also have a higher affinity, allowing one to balance expression, repression and length-preference. Although plasmid-based assays ultimately have different mass action kinetics to single-copy target chromosomal assays, they allowed us to verify our hypothesis rapidly before moving onto chromosomal targets.

ZFxHunt of different lengths were therefore tested using reporter vectors with N-terminal CAG repeats from the human *HTT* gene in frame with EGFP (Q0, Q10, Q35 and Q104; Q=CAG). To assess non-specific effects, an HcRed reporter was cloned in a different region of the same vector, under an independent promoter (Fig. 2A). HEK293T cells were transiently co-transfected with the indicated reporter and ZFxHunt vectors, driven by CMV promoters. As gene therapy delivery vectors (used later) have a limited packaging capacity, which is exceeded by 12-fingers, we also tested an 11-finger construct. We found a similar expression levels and activity

between ZF12xHunt and ZF11xHunt (Fig. S1), and so used ZF11xHunt in all subsequent assays.

Three assays were used to measure ZFxHunt repression: quantifying EGFP and HcRed fluorescent cells using Fluorescence-Activated Cell Sorting (FACS), EGFP protein levels in Western blots, and EGFP and HcRed mRNA levels in qRT-PCR (Fig. 2B-D). In these experiments, ZFxHunt with 6-, 11- and 18- fingers all repressed the two longer CAG-repeats strongly (5-9-fold: 80-90% repression) whereas ZF4xHunt was slightly weaker (2-4-fold: 50-75% repression). A Student's t-test analysis revealed that ZF11xHunt gave significant repression of longer polyQ reporter genes the most consistently out of all ZF constructs, with no significant unspecific repression of the HcRed controls (p-values in Supplementary Tables S1,2). Verifying that the results were not specific to ZFP under the CMV promoter, similar results were obtained with the phosphoglycerate kinase (PGK) promoter (Fig. S2). Although binding interactions (and thus particular length-preference) can always be modulated by changing the effective concentration of each species, the main conclusion that can be drawn here is that there is a positive relationship between CAG repeat number and repression level. Furthermore, ZF6-, ZF11- and ZF18xHunt are all strong repressors of longer repeats under these conditions.

Competition assays show preferential repression of long CAG-repeats by ZFxHunt. Up to this point, the zinc fingers had displayed length preference for single CAG-repeat targets in cells. Another test of potential length-preference is for discrimination against two targets per cell, each with a different number of CAG-repeats. HEK293T cells were therefore co-transfected with three plasmids: the indicated polyQ-EGFP and polyQ-mCherry reporter vectors, together with various ZFxHunt vectors (Fig. 3). The relative expression of the two reporters was measured by FACS (EGFP or mCherry positive cells). Figure 3 shows that the longer CAG-repeats are preferentially repressed by all ZFxHunt, so that cells are dominated by the shorter green or red constructs when their opposite counterpart is longer; this is seen directly by looking at the ratio of green-to-red expression. This can be explained most simply by mass action (longer CAG-repeats contain more target sites, so are bound and repressed more).

This assay demonstrates the potential of ZFxHunt for CAG-length discrimination. Therefore length preference exists, even for multiple different-length CAG-repeats within the same cell. The remaining caveat is that the system still needs to be tailored (expression levels, zinc finger length, repression strength) for the particular cellular environment. We therefore moved next to testing in a more physiological chromosomal cellular environment.

Chromosomal repression of mutant *HTT* in a HD model cell line. Since ZF4xHunt had weaker binding and length preference (Fig. 2, 3), and since ZF12- and ZF18xHunt are beyond the packaging limit of AAV, we focussed on testing ZF6xHunt and ZF11xHunt, on chromosomal *HTT* genes. ST*Hdh* cells (34) are an established neuronal progenitor cell line from E14 striatal primordia, derived from wt mice (STHdh^{Q7}/Hdh^{Q7}), or knock-ins, where the first exon of the mouse *HTT* gene has been replaced by a human exon with 111 CAG repeats (STHdh^{Q111}/Hdh^{Q111} or STHdh^{Q7}/Hdh^{Q111}). Because the chromosomal targets are present at a much lower effective concentration, to increase the repression per binding event we also tested an effector domain in parallel: the Kox-1 KRAB domain (35).

ST*Hdh* cells stably expressing 'naked' or Kox-1-fused ZF6xHunt and ZF11xHunt were harvested 20 days after retroviral infection, and huntingtin levels were analyzed by Western blot and qRT-PCR (Fig. 4A). Neither protein nor RNA levels of wt *HTT* (Q7) were reduced by naked or Kox-1-fused ZF6xHunt and ZF11xHunt. By contrast, Q111-mutant *HTT* RNA and protein levels were repressed with ZF6xHunt-Kox-1 by up to 2.5-fold (60% reduction) and 2-fold (50% reduction), respectively. Similar results were achieved in Q7/Q111 heterozygous cells (Fig. S3). ZF11xHunt-Kox-1 showed even stronger repression, with almost 80% reduction in mRNA expression and 95% reduction in the protein levels. Overall, the longer 11-finger construct, together with stronger Kox-1 repression, displayed the strongest chromosomal repression of mut *HTT*.

ZFxHunt does not repress wt CAG-containing genes. Genomes contain several other endogenous CAG repeat genes, and so the potential side-effects of stably-

expressed ZFxHunt proteins were assayed by qRT-PCR for atrophin1, ataxin-1, ataxin-2, ataxin-3, ataxin-7, calcium channel alpha 1A subunit, and TATA binding protein (Fig. 4B-D). No strong effects were seen in either ST*Hdh* mouse cells (Fig. 4B), or in HEK293T cells (with counterpart human PCR primers)(Fig. 4C). In the latter, even genes with relatively long repeats were unaffected (human *HTT*, 21-repeats; *Tbp* ~38-repeats: 36 CAG repeats broken by two non consecutive CAA codons; Table S3).

As Kox-1 recruits the co-repressor KAP-1 and induces long-range repression through the spread of heterochromatin (36), we tested the effects of ZF6xHunt-Kox-1 and ZF11xHunt-Kox-1 on genes neighboring *HTT*, in stably-transduced ST*Hdh* cells, by qRT-PCR (Fig. 4B). The two adjacent genes, G protein-coupled receptor kinase 4 (~7 kb upstream) and G-protein signaling 12 (~188 kb downstream), were both unchanged, suggesting that they are out of range. Thus, ZF6- and ZF11xHunt-Kox-1 repression appears to be specific for mutant *HTT* in chromosomal loci. Additionally, a dye-labeling cell viability assay (Fig. S4) revealed no statistically significant toxic effects, encouraging us to test the ZFP's potential *in vivo*.

ZF11xHunt-KoxI represses *HTT* in a HD patient cell line. Since HD patients typically have CAG-repeats in the 42-45 range, we tested the potential for repression of these shorter targets in a patient-derived mesothelial cell line (Q45/Q21). We again observed that other genomic CAG-repeat genes remained unaffected, while *HTT* was repressed (Fig. 4D). The Q45/Q21 line is heterozygous and, based on the other repression data, we only expect the Q45 allele to be repressed under these conditions. 100% repression of only the mutant allele would give a maximum 2-fold repression of *HTT* in this assay. In fact we observe a ~1.8-fold repression of *HTT* (Fig. 4D). As the other shorter CAG-repeat genes (including the split 38-repeat *Tbp*) are not repressed, this indicates that selective inhibition of mutant repeats at the shorter end of the pathological spectrum is possible.

ZFxHunt fused to Kox-1 reduces expression of mutant *HTT in vivo*. Although ZF11xHunt-Kox-1 apparently functioned well in the stable transfection with dividing cells, this system is quite different from the environment of a mammalian brain,

where there are many cell types and most of them are non-dividing. We therefore decided to test whether any repression could be observed in a more physiological setting.

rAAV pseudotype 2/1 (AAV2/1), containing AAV2 terminal repeats and AAV1 capsid, efficiently transduces neurons (and most glial and some ependymal cells) and appears to be the most efficient pseudotype for transducing large volumes of the striatum (37). R6/2 mice are one of the most-widely used models of HD because they show highly reproducible early onset symptoms, allowing the use of fewer animals (38). Although R6/2 have very long CAG-repeats (range 115-160), which are rarely found in patients (typically in the 42-45 range), they are nonetheless ideal to assay acute phenotypic reversal at the molecular, histologic and early-symptom levels (39). Therefore, R6/2 mice were stereotaxically injected at 4 weeks of age with AAV2/1 expressing ZF11xHunt-Kox-1.

We initially tested vectors expressing the ZF under a CMV promoter, but we observed very low levels of expression of the ZF protein and mRNA, and no repression of mutant *HTT*. CMV promoters can be quickly silenced by DNA methylation (40), whereas high and persistent levels of expression can be achieved in the central nervous system with rAAV using the CAG promoter (CMV enhancer, chicken beta-actin hybrid promoter) and a WPRE (Woodchuck hepatitis virus postranscriptional regulatory element) (41, 42). We therefore produced a second generation of rAAV using these elements.

CAG-WPRE constructs were injected into the striatum of one brain hemisphere, with AAV2/1-GFP control injections (equal titre) into the other. ZFP striatal expression was confirmed by Western blot (Fig. S5A), while GFP fluorescence shows transduction of large striatal volumes (Fig. 5A). For parallel behavioural studies, both hemispheres were injected (Fig. 5B), also resulting in high and reproducible expression (Fig. 5C). The cellular targeting of AAV2/1 was assayed by immunohistochemistry, showing that transgene expression coincides with a neuronal cell marker as previously shown in Ref. (37) (Fig. S6CDE).

Two weeks after injection, the mice were sacrificed and brain *HTT* levels were analysed by qRT-PCR (Fig. 6A,B). The levels of mutant *HTT* transgene mRNA were reduced in the striatum by 40% on average (up to 60% in individual mice), as compared to the control hemispheres ($p = 0.006$). Furthermore, both the non-injected cerebellum and wt *HTT* were unaffected (Fig. 6A). A linear regression analysis, comparing expression levels of ZFxHunt-Kox-1 mRNA with those of mutant *HTT,* showed that they correlated closely and negatively ($r = 0.83$; $p = 0.02$) (Fig. 6B). Aggregates of mutant HTT protein were detected with anti-HTT antibodies (Fig. 6C), also showing a significant reduction (~40%) in the treated striatum (Fig. 6D; Student's t test for paired samples, $p=0.03$; Fig. S7, S8). Again, mutant HTT did not change significantly in the non-injected cortex (Fig. 6C,D).

Neither striatal volume nor cell density in the striatum was affected by treatment or genotype, indicating that the reduction of mutant HTT was not due to a loss of cells and providing no evidence of ZFxHunt toxicity at this level (ANOVA, Genotype $p>0.1$; Treatment $p>0.1$)(Table S4). Overall, these data are consistent with *in vivo* dose-dependent repression of mutant *HTT* by the zinc finger construct.

The results demonstrate acute mutant *HTT* repression by zinc fingers in the mouse brain. Therefore, we tested *in vivo* if the molecular changes observed in the brain would translate to beneficial effects on the pathology phenotype of the R6/2 HD mouse model.

First, we investigated whether the zinc finger repression improved the HD phenotype, using a standard assay where HD-mice display a clasping behaviour when lifted by the tail (43) (Fig. 7A). In a double blind experiment, male R6/2 mice were injected bilaterally in the striata, at 4 weeks of age, with AAV2/1-ZF11xHunt-Kox-1 or AAV2/1-GFP. A control group was left un-operated. Strikingly, the AAV2/1-ZF11xHunt-Kox-1 injected mice showed an almost complete absence of diseased clasping behaviour (Fig. 7B). While control R6/2 mice started displaying clasping as early as week 4, ZF-treated R6/2 mice did not clasp until week 7. Even then, only 1/8 ZF-treated mice clasped, compared to 6/12 control R6/2 mice (Chi-square test,

p=0.03). GFP-treated R6/2 mice did not differ from un-operated controls (p > 0.7)(Fig. 7B).

To assess motor coordination, male R6/2 mice and their wt littermates were tested at 3 weeks of age for their baseline performance (latency to fall) in the accelerating rotarod test. They subsequently received bilateral striatal injections at 4 weeks, as described above. Repeated measures ANOVA comparing the decline in R6/2 performance revealed that GFP-treated R6/2 were significantly impaired as compared to their GFP-treated wt controls (p=0.035), whereas the AAV2/1-ZF11xHunt-Kox-1 treated R6/2 mice not different from the wt mice (p>0.1)(Fig. 7C).

In our experiments, R6/2 mice do not experience any weight-loss or changes in survival compared to their wt counterparts and thus these phenotypes cannot be used as endpoints. We did not observe any significant difference in weight between wt and R6/2, treated and untreated mice (Fig. S9) and no mice died during the experiment, either with or without treatment, so no conclusion can be drawn about the effect of treatment on these phenotypes.

The data presented establish a proof-of-principle that zinc finger repressors can be active after striatal delivery, with *HTT* reduction at the RNA and protein level, and significant improvements in disease phenotypes in a HD mouse model.

Discussion

In this study, we have described the design of a ZFP able to recognize and bind both DNA strands of a stretch of CAG repeats, by recognizing both poly-GCA and -GCT triplets, to induce transcription repression. As shown in Figure 2, even naked ZFxHunt are highly efficient episomally and can reduce polyQ-EGFP expression by up to 90%. The mechanism of repression here is likely to be steric hindrance of RNA polymerase complex progression, as reported by Choo et al. for a synthetic ZFP against the bcr-abl oncogene (44). By contrast, in chromosomal loci, the stronger repression conferred by the Kox-I repression domain (35, 36) is required to see an effect (Figure 4).

One major *in vitro* observation was that longer CAG-repeats were repressed more by particular finger constructs under given conditions, suggesting that mass action can be exploited to give a degree of length preference. Binding to different lengths of CAG-repeats is, of course, altered by the effective concentrations of both zinc finger and target. We therefore had to find empirically which length of zinc finger and which expression construct would give an effective dose to discriminate between the lengths of CAG-repeats in a chosen HD mouse model.

By first using a model cell line derived from striatial cells of a knock-in HD mouse model (the full *HTT* gene, with variable CAG-repeats in exon 1) (34), we found effective constructs and doses which gave a great deal of specificity for repressing mutant Huntingtin at a chromosomal level. Although repression of the shorter wt HTT protein is well tolerated for several months in animal models (14, 45), it is desirable to preferentially target the mutant allele (13, 16), and one should not affect other CAG-repeat containing genes. In fact, under the dosages tested, we found conditions in which mutant *HTT* was strongly repressed for a sustained period of 20 days, with no apparent side-effects on other shorter CAG-repeat genes. Therefore the next step was to explore whether repression could also be achieved in the brain, using gene therapy vectors for delivery.

Gene therapy is an attractive therapeutic strategy for various neurodegenerative diseases. For example, lentiviral vectors have been used to mediate the widespread and long-term expression of transgenes in non dividing cells such as mature neurons (46). A rAAV vector was also used by Rodriguez-Lebron et al. (47) to deliver anti-mutant *HTT* shRNAs in HD model mice, thereby reducing striatal mutant *HTT* levels and slowing progression of the HD-like phenotype. As outlined in the introduction, several strategies to target *HTT* have shown promise (11-13, 16, 17, 19). However, repression in the brain by a synthetic transcription factor has never been reported. It was unknown whether sufficient levels of protein could be produced after *in vivo* delivery to see any repression, whether transcription repression would be sufficient to reduce protein levels, and whether such constructs would show acute toxicity. In fact, we were able to get effective repressors that were well-tolerated, but this required a degree of further optimisation, including the use of a strong CAG promoter and

WPRE (42). With these improvements we observed selective repression of mutant *HTT* RNA, a reduction in HTT protein aggregates and an alleviation of associated HD phenotypic deficits.

Overall, the results presented in this study establish a proof-of-principle that ZFs can acutely repress mutant *HTT in vivo* via striatal injection, in a dose-dependent manner. These results imply that it is worth pursuing these constructs to test a multitude of possible gene therapy vector and zinc finger variants, with a view to optimising potential therapeutic benefit.

Materials and Methods

Vectors. To build a ZFP that recognizes both GCA and GCT DNA sequences, we based our designs on two previous studies. Choo et al. (44) engineered ZFPs with the following alpha-helical recognition sequences: QAATLQR for GCA, and QAQTLQR for GCT. Isalan et al. (48), showed that QRASRKR recognizes GN (T/A). Therefore we proposed a hybrid design, QRATLQR (ZFxHunt), for GC (T/A) (Fig. 1c). A pUC56 vector containing ZF6xHunt was synthesised by Genscript Corporation (Piscataway, NJ). This vector included a T7 promoter, zif268 DNA-binding domain backbone, an N-terminal NLS (PKKKRKV), and restriction sites for deriving ZF4, 12 and 18 by subcloning (full sequences given in Supplementary Information).

ZF6xHunt was subcloned into the mammalian expression vector pTarget (Promega). A 3xFLAG tag sequence (DYKDHDG DYKDHDI DYKDDDDK) was introduced by PCR at the N-terminus, and either FokI endonuclease domain or Kox-1 (KRAB repression domain) coding sequences were introduced at the C-terminus, with a 3xGGGGS linker.

The pEH vector series was cloned in two steps. First, EGFP coding region was excised from pEGFP-N1 (Clontech), using HindIII/XbaI, and cloned into pGL4.13 (Promega) to give pSV40-EGFP. Then, a PCR product containing CMV-HcRed-polyA and ClaI linkers was cloned into pSV40-EGFP (partially digested with ClaI).

The EGFP start codon was mutated to Alanine by site directed mutagenesis, and PCR fragments containing human *HTT* exon I from different human genomic templates (to obtain different number of CAG repeats) were cloned into the pEH EcoRI site, upstream and in frame with EGFP (pEH-Q series). The pSV40-mCherry vector series were generated by replacing EGFP from the pSV40-EGFP vector series by mCherry using XmaI/XbaI sites.

Gel Shift. pUC56-ZFxHunt and M13 and M13rev primers were used to generate PCR products for in vitro expression of the indicated ZFP, using the TNT T7 Quick PCR DNA kit (Promega). Double stranded DNA probes with different number of CAG repeats with the standard sequence ACG TAC (CAG)x TCA CAG TCA GTC CAC ACG TC were produced by Klenow fill-in. 100 ng of double stranded DNA were used in a DIG-labeling reaction using Gel Shift kit, 2nd generation (Roche) following manufacturer's instructions. For gel shift assays, 0.005 pmol of DIG-labelled probe were incubated with increasing amounts of TNT-expressed protein in a 20 µl reaction containing 0.1 mg/ml BSA, 0.1 µg/ml polydI:dC, 5% glycerol, 20 mM Bis-Tris Propane, 100 mM NaCl, 5 mM $MgCl_2$, 50 mg/ml $ZnCl_2$, 0.1% NonidetP40 and 5 mM DTT for 1 h at 25˚C. Binding reactions were separated in a 7% non-denaturing acrylamide gel for 1 h at 100 V, transferred to a nylon membrane for 30 min at 400 mA, and visualization was performed following manufacturer's instructions.

Cell culture and gene delivery. The cell line HEK293T (ATCC) was cultured in 5% CO_2 at 37˚C in DMEM (Gibco) supplemented with 10% FBS (Gibco). Qiagen purified DNA was transfected into cells using Lipofectamine 2000 (Invitrogen) according to manufacturer's instructions. Briefly, cells were plated onto 10 mm wells to a density of 50% and 70 ng of reporter plasmid, 330 ng of ZFP expression plasmid and 2 µl of Lipofectamine 2000 were mixed and added to the cells. Cells were harvested for analysis 48 hours later. All assays were performed in triplicate. ST*Hdh+/Hdh+* and ST*HdhQ111/Hdh111* cells (gift from M.E. MacDonald) were cultured in 5% CO_2 at 33˚C in DMEM supplemented with 10% FBS (Gibco) and 400 µg/ml G418 (PAA). *Q45/Q21 patient-derived cell line:* mesothelial cells from a heterozygous HD patient (Q45/Q21) were collected from urine and cryopreserved with glycerol. After thawing, surviving cells were grown in Chang Medium D. Cells

were infected with retroviral particles using the pRetroX system (Clontech) according to manufacturer's instructions. Samples were FACS sorted for GFP expression 7 days after transduction, and allowed to recover for 2 weeks before extracting RNA or protein for qRT-PCR and Western blot.

Flow cytometry analysis. Cells were harvested 48 h post-transfection and analyzed in a BD FACS Canto Flow cytometer using BD FACSDiva software.

Western blot. 293T cells were harvested 48 hours post-transfection in 100 µl of 2xSDS loading dye with Complete protease inhibitor (Roche). 20µl of sample were separated in 4-15% Criterion Tris-HCl ready gels (BioRad) for 2 h at 100V, transferred to Hybond-C membrane (GE Healthcare) for 1 h at 100V. Proteins were detected with either the primary antibody anti β-actin (Sigma A1978) at 1:3 000 dilution or Anti-EGFP (Roche) at 1:1,500 dilution and with a Peroxidase-conjugated Donkey anti-mouse secondary antibody (Jackson ImmunoResearch) at 1:10 000 dilution. Visualization was performed with ECL system (GE Healthcare) using a LAS-3000 imaging system (Fujifilm). ST*Hdh* cells (from one ~80% confluent 15 cm plate) were trypsinized and harvested in PBS containing Complete protease inhibitor (Roche). Cells were resuspended in RIPA buffer (1% TritonX-100, 1% sodium deoxycholate, 40 mM Tris-HCl, 150 mM NaCl, 0.2% SDS, Complete), incubated in ice for 15 min, and were centrifuged at 13.000 rpm for 15 min. The supernatant was collected and protein concentration was determined using BioRad's D_C protein assay. 60 µg of protein were separated in a 5% Criterion Tris-HCl ready gel (BioRad) for 2 hours at 100V, transferred using iBlot Dry Blotting System (Invitrogen) for 8 min and endogenous HTT protein was detected with anti-Huntingtin primary antibody (Millipore MAB2166) at a 1:1 000 dilution.

qRT-PCR. RNA from cells in one well of an ~80% confluent 24-well plate was prepared with RNeasy kit (Qiagen) and 500ng (unless indicated) were reversed transcribed with Superscript II (Invitrogen). Real Time PCR was performed in a LightCycler® 480 Instrument (Roche) using LightCycler® 480 SYBR Green I Master (Roche). SYBR Advantage GC qPCR Premix (Clontech) was used to amplify the human *HTT* transgene in R6/2 templates. For technical replicates, each PCR was done

in triplicate, and results normalized to three housekeeping genes. At least 3 independent biological replicates (or as indicated if different) were done for each experiment. Primer sets are given in full in Table S3.

Production of Adeno-Associated Viral Vector. AAV2/1-CAG-GFP-WPRE and AAV2/1-CAG-ZF11xHunt-KoxI-WPRE, containing a CAG promoter (CMV early enhancer element and the chicken beta-actin promoter) and WPRE (Woodchuck post-translational regulatory element) were produced at the Centre for Animal Biotechnology and Gene Therapy of the Universitat Autonoma of Barcelona (CBATEG-UAB) as previously described (49). Recombinant virus was purified by precipitation with PEG8000 followed by iodixanol gradient ultracentrifugation with a final titer of 7.41×10^{11} genome copies/ml.

Animals. R6/2 transgenic mice were purchased form Jackson Laboratories (B6CBA-Tg(HDexon1)62Gpb/3J). Ovarian transplanted hemizygous females and wt B6CBAF1/J males were bred in house, and progeny was genotyped as previously described (50). Stereotaxic injections were performed on 4-week-old mice. Briefly, mice were anesthetized with a mix of ketamine (75 mg/kg) and medetomidine (1 mg/kg, i.p.) and fixed on a stereotaxic frame. Analgesia was provided by buprenorphine (8 μg/kg, s.c.). AAVs were injected bilaterally into the striatum (A/P +0.7 mm, M/L ± 1.8 mm, D/V –3.0 mm relative to bregma) using a 10 µl Hamilton syringe at a rate of 0.25 µl/min controlled by an Ultramicropump (World Precision Instruments). For each hemisphere, a total volume of 3 µl ($2.2x10^9$ genomic particles) were injected in two steps: 1.5 µl were injected at –3.0 mm DV, the needle was let to stand for 3 minutes in position, and then the other half was injected at –2.5 mm DV. Mice were randomly injected with AAV2/1-CAG-ZF11xHunt-Kox-1-WPRE in one hemisphere and with control AAV expressing GFP into the other hemisphere. Some mice were injected only in one hemisphere with AAV2/1-ZF for comparison to non-injected control hemisphere. Mice were sacrificed after 2 weeks for posterior analysis by RT-PCR (primers: mut *HTT*, n=6; wt *HTT*, n=9*;* ZF-Kox, n=9) and histological analyses (WT, n=3; R6/2, n=3).

Histology. Mice were killed with CO_2 and rapidly transcardially perfused with saline solution, followed by 75 ml of 4% paraformaldehyde in 0.01 M phosphate-buffered saline (PBS). Hemispheres were separated and post-fixed in the same fixative o.n. at 4ºC and immersed in 30% sucrose-PBS until they sank. Hemibrains were frozen in a freezing microtome cryostat and 40 μm-thick coronal sections were obtained. Freefloating sections were collected in six parallel series. One section was stained with Hematoxilin-eosin for calculation of the volume of the striatum in both R6/2 and WT mice. A second section was processed for immunocytochemical detection of human mutant huntingtin. As controls, we used a mix of slices from wt mice following the whole immunodetection, as well as one slice per hemisphere and R6/2 mouse not incubated with the primary antibody. The rest of the series were frozen in cryoprotectant solution for further use.

Briefly, sections were incubated sequentially in: (i) 1% hydrogen peroxide (H_2O_2) in TBS for 30 min at room temperature, for endogenous peroxidase inactivation; (ii) mouse anti-mut HTT (Millipore MAB5374) diluted 1 : 100 in TBS with 0.3% Triton X-100 (Sigma, St. Louis, MO, USA) and 2% normal goat serum (NGS, Vector Laboratories, Burlingame, CA, USA), overnight at 4 ºC; (iii) biotinylated goat anti-mouse IgG (Vector Laboratories) diluted 1 : 200 in TBS with 0.3% Triton X-100 and 2% NGS for 2 h at room temperature; and (iv) avidin–biotin–peroxidase complex (ABC Elite Kit; Vector Laboratories) in TBS with 0.3% Triton X-100, for 90 min at room temperature. Following each incubation, sections were washed in TBS (3x5 min). The resulting peroxidase activity was revealed with FAST diaminobenzidine (Sigma) for 5 min. Sections were rinsed in TBS and mounted onto slides, cleared with xylene, and coverslips were fixed with Permount. For Neu-N detection, slices were (i) incubated o.n. at 4º with anti-neu-N (Millipore MAB377) (ii) goat-anti-mouse-Alexa-555 (Invitrogen A21422).

Image analysis

Determination of the volume and cell density of the striatum. Striatal volume was determined using the software Computer Assisted Stereology Toolbox (CAST) (Olympus Danmark, A/S) according to the principle of Cavalieri (volume=$s_1d_1+s_2d_2+\ldots.s_nd_n$) (51) considering 8 coronal levels from bregma 1.5 mm (following the mouse brain atlas (52)) and an interval of 240 µm between the

sections. Cell density was calculated in the same slices using the unbiased optical dissector method (53).

Automatic count of mut HTT *positive particles*. In the mut HTT immunostained series, 4 coronal slices per R6/2 mouse and hemisphere from bregma 1.5 levels were selected, and a region of interest of 650 x 865 μm^2 in the middle of dorsal striatum captured with a 10X objective using a digital camera attached to a Olympus BX51 microscope. ImageJ software (NIH) was used for image analysis. Following the method of Ref. (52)(Fig. S7), counts were obtained and calculated per 0.1 mm^2. This gave the number of mut HTT immunoreactive particles in the 4 slices of both cerebral hemispheres and the number of particles averaged providing a single density measure per mouse.

Clasping assay. R6/2 males were bilaterally injected with 3 μl of the same virus in both hemispheres for behavioral assays. Behavioral monitoring was carried out from 4 to 7 weeks of age. All the experiments were blindly performed with respect to the treatment of the mice (R6/2 mice: un-operated, n=8, ZFP-treated n=8; GFP-mock treated, n=4). Animals were assessed for clasping behaviour by suspending them by their tails for 20 seconds. Mice clasping their hindlimbs were given a score of 1 and mice that did not clasp, 0.

Accelerating rotarod. Mice (R6/2 mice: ZFP-treated n=12; GFP-mock treated, n=12; WT mice: ZFP-treated n=14; GFP-mock treated, n=14) were trained at week 3 of age to stay on the rod at a constant speed of 4 r.p.m. until they reached a criterion of 3 consecutive minutes on it. In the testing phase, mice were put in the rotarod at 4 r.pm. and the speed was constantly increased for 2 minutes to 40 r.p.m. The assay was repeated twice and the maximum latency to fall from the rod was recorded. Decline in performance was calculated as the difference in the latency to fall from pre-surgery levels with respect to weeks 5 and 7.

Statistical analysis. Error bars in figures are one standard error based on at least three biological replicates. Data of the repression of polyQ reporter genes experiments were analysed using a Student's t test against an expected value of 1 (no repression or activation). Expected percentages of mice clasping were inferred of our population of

un-operated R6/2 mice, and a Chi-square test for goodness-of-fit was applied to the observed percentages in operated groups. Data of the accelerating rotarod test were analyzed using repeated measures ANOVA with week as within-subject factor and group as between-subject factor, followed by a post-hoc analysis using the Bonferroni correction.

Acknowledgments

We thank L. Serrano and B. Lehner for critical reading, and M.E. MacDonald for the ST*Hdh+/Hdh+* and ST*HdhQ111/Hdh111* cells. We dedicate this work to Max Perutz for providing inspiration on polyglutamines.

Funding disclosure

MI is funded by FP7 ERC 201249 ZINC-HUBS, Ministerio de Ciencia e Innovacion grant MICINN BFU2010-17953 and MD is funded by SAF2010-16427, and the MEC-EMBL agreement. The funders had no role in study design, data collection and analysis, decision to publish, or preparation of the manuscript.

Author Contribution

MGC and MI designed the project. MGC performed *in vitro* assays, cells assays and gene therapy assays in mice. CAP performed gene therapy, behavioral tests in and histology experiments in mice. FH contributed to cell assays. AS developed the Q45 patient cell line. CFF contributed to the design of the gene delivery vector. MD contributed to the design of the behavioral assays. MGC, CAP and MI wrote the manuscript.

Ethics statement

Animal handling procedures was conducted in accordance with Directive 86/609/EU of the European Commission and following protocols approved by the Ethical Committee of the Barcelona Biomedical Research Park.

References

1. Walker FO (2007) Huntington's Disease. Semin Neurol 27(2):143-150.
2. Orr HT & Zoghbi HY (2007) Trinucleotide repeat disorders. Annu Rev Neurosci 30:575-621.
3. Cha JH (2007) Transcriptional signatures in Huntington's disease. Prog Neurobiol 83(4):228-248.
4. Kumar P, Kalonia H, & Kumar A (2010) Huntington's disease: pathogenesis to animal models. Pharmacol Rep 62(1):1-14.
5. The-Huntington's-Disease-Collaborative-Research-Group (1993) A novel gene containing a trinucleotide repeat that is expanded and unstable on Huntington's disease chromosomes. The Huntington's Disease Collaborative Research Group. Cell 72(6):971-983.
6. Ramaswamy S & Kordower JH (2012) Gene therapy for Huntington's disease. Neurobiol Dis.
7. Sharp AH*, et al.* (1995) Widespread expression of Huntington's disease gene (IT15) protein product. Neuron 14(5):1065-1074.
8. Duyao MP*, et al.* (1995) Inactivation of the mouse Huntington's disease gene homolog Hdh. Science 269(5222):407-410.
9. Dragatsis I, Levine MS, & Zeitlin S (2000) Inactivation of Hdh in the brain and testis results in progressive neurodegeneration and sterility in mice. Nat Genet 26(3):300-306.
10. Matsui M & Corey DR (2012) Allele-selective inhibition of trinucleotide repeat genes. Drug Discov Today.
11. van Bilsen PH*, et al.* (2008) Identification and allele-specific silencing of the mutant huntingtin allele in Huntington's disease patient-derived fibroblasts. Hum Gene Ther 19(7):710-719.
12. Zhang Y, Engelman J, & Friedlander RM (2009) Allele-specific silencing of mutant Huntington's disease gene. J Neurochem 108(1):82-90.
13. Pfister EL*, et al.* (2009) Five siRNAs targeting three SNPs may provide therapy for three-quarters of Huntington's disease patients. Curr Biol 19(9):774-778.
14. Grondin R*, et al.* (2012) Six-month partial suppression of Huntingtin is well tolerated in the adult rhesus striatum. Brain.
15. McBride JL*, et al.* (2011) Preclinical safety of RNAi-mediated HTT suppression in the rhesus macaque as a potential therapy for Huntington's disease. Mol Ther 19(12):2152-2162.
16. Hu J*, et al.* (2009) Allele-specific silencing of mutant huntingtin and ataxin-3 genes by targeting expanded CAG repeats in mRNAs. Nat Biotechnol 27(5):478-484.
17. Hu J, Matsui M, & Corey DR (2009) Allele-selective inhibition of mutant huntingtin by peptide nucleic acid-peptide conjugates, locked nucleic acid, and small interfering RNA. Ann N Y Acad Sci 1175:24-31.
18. Kordasiewicz HB*, et al.* (2012) Sustained therapeutic reversal of Huntington's disease by transient repression of huntingtin synthesis. Neuron 74(6):1031-1044.
19. Bauer PO*, et al.* (2010) Harnessing chaperone-mediated autophagy for the selective degradation of mutant huntingtin protein. Nat Biotechnol 28(3):256-263.
20. Klug A (2009) The Discovery of Zinc Fingers and Their Applications in Gene Regulation and Genome Manipulation. Annu Rev Biochem.

21. Pabo CO, Peisach E, & Grant RA (2001) Design and selection of novel Cys2His2 zinc finger proteins. Annu Rev Biochem 70:313-340.
22. Jantz D, Amann BT, Gatto GJ, Jr., & Berg JM (2004) The design of functional DNA-binding proteins based on zinc finger domains. Chem Rev 104(2):789-799.
23. Sera T & Uranga C (2002) Rational design of artificial zinc-finger proteins using a nondegenerate recognition code table. Biochemistry 41(22):7074-7081.
24. Mandell JG & Barbas CF, 3rd (2006) Zinc Finger Tools: custom DNA-binding domains for transcription factors and nucleases. Nucleic Acids Res 34(Web Server issue):W516-523.
25. Kim JS, Lee HJ, & Carroll D (2010) Genome editing with modularly assembled zinc-finger nucleases. Nat Methods 7(2):91; author reply 91-92.
26. Kim HJ, Lee HJ, Kim H, Cho SW, & Kim JS (2009) Targeted genome editing in human cells with zinc finger nucleases constructed via modular assembly. Genome Res 19(7):1279-1288.
27. Hurt JA, Thibodeau SA, Hirsh AS, Pabo CO, & Joung JK (2003) Highly specific zinc finger proteins obtained by directed domain shuffling and cell-based selection. Proc Natl Acad Sci U S A 100(21):12271-12276.
28. Wright DA*, et al.* (2006) Standardized reagents and protocols for engineering zinc finger nucleases by modular assembly. Nat Protoc 1(3):1637-1652.
29. Maeder ML*, et al.* (2008) Rapid "open-source" engineering of customized zinc-finger nucleases for highly efficient gene modification. Mol Cell 31(2):294-301.
30. Mittelman D*, et al.* (2009) Zinc-finger directed double-strand breaks within CAG repeat tracts promote repeat instability in human cells. Proc Natl Acad Sci U S A 106(24):9607-9612.
31. Moore M, Klug A, & Choo Y (2001) Improved DNA binding specificity from polyzinc finger peptides by using strings of two-finger units. Proc Natl Acad Sci U S A 98(4):1437-1441.
32. Kim JS & Pabo CO (1998) Getting a handhold on DNA: design of poly-zinc finger proteins with femtomolar dissociation constants. Proc Natl Acad Sci U S A 95(6):2812-2817.
33. Miller J, McLachlan AD, & Klug A (1985) Repetitive zinc-binding domains in the protein transcription factor IIIA from Xenopus oocytes. EMBO J 4(6):1609-1614.
34. Trettel F*, et al.* (2000) Dominant phenotypes produced by the HD mutation in STHdh(Q111) striatal cells. Hum Mol Genet 9(19):2799-2809.
35. Margolin JF*, et al.* (1994) Kruppel-associated boxes are potent transcriptional repression domains. Proc Natl Acad Sci U S A 91(10):4509-4513.
36. Groner AC*, et al.* (2010) KRAB-zinc finger proteins and KAP1 can mediate long-range transcriptional repression through heterochromatin spreading. PLoS Genet 6(3):e1000869.
37. Burger C*, et al.* (2004) Recombinant AAV viral vectors pseudotyped with viral capsids from serotypes 1, 2, and 5 display differential efficiency and cell tropism after delivery to different regions of the central nervous system. Mol Ther 10(2):302-317.
38. Crook ZR & Housman DE (2012) Dysregulation of dopamine receptor D2 as a sensitive measure for Huntington disease pathology in model mice. Proc Natl Acad Sci U S A 109(19):7487-7492.

39. Gil JM & Rego AC (2009) The R6 lines of transgenic mice: a model for screening new therapies for Huntington's disease. Brain Res Rev 59(2):410-431.
40. Migliaccio AR*, et al.* (2000) Stable and unstable transgene integration sites in the human genome: extinction of the Green Fluorescent Protein transgene in K562 cells. Gene 256(1-2):197-214.
41. Garg S, Oran AE, Hon H, & Jacob J (2004) The hybrid cytomegalovirus enhancer/chicken beta-actin promoter along with woodchuck hepatitis virus posttranscriptional regulatory element enhances the protective efficacy of DNA vaccines. J Immunol 173(1):550-558.
42. Tenenbaum L*, et al.* (2004) Recombinant AAV-mediated gene delivery to the central nervous system. J Gene Med 6 Suppl 1:S212-222.
43. Reddy PH*, et al.* (1999) Transgenic mice expressing mutated full-length HD cDNA: a paradigm for locomotor changes and selective neuronal loss in Huntington's disease. Philos Trans R Soc Lond B Biol Sci 354(1386):1035-1045.
44. Choo Y, Sanchez-Garcia I, & Klug A (1994) In vivo repression by a site-specific DNA-binding protein designed against an oncogenic sequence. Nature 372(6507):642-645.
45. Boudreau RL*, et al.* (2009) Nonallele-specific silencing of mutant and wild-type huntingtin demonstrates therapeutic efficacy in Huntington's disease mice. Mol Ther 17(6):1053-1063.
46. Dreyer JL (2010) Lentiviral vector-mediated gene transfer and RNA silencing technology in neuronal dysfunctions. Methods Mol Biol 614:3-35.
47. Rodriguez-Lebron E, Denovan-Wright EM, Nash K, Lewin AS, & Mandel RJ (2005) Intrastriatal rAAV-mediated delivery of anti-huntingtin shRNAs induces partial reversal of disease progression in R6/1 Huntington's disease transgenic mice. Mol Ther 12(4):618-633.
48. Isalan M, Klug A, & Choo Y (1998) Comprehensive DNA recognition through concerted interactions from adjacent zinc fingers. Biochemistry 37(35):12026-12033.
49. Salvetti A*, et al.* (1998) Factors influencing recombinant adeno-associated virus production. Hum Gene Ther 9(5):695-706.
50. Benn CL*, et al.* (2009) Genetic knock-down of HDAC7 does not ameliorate disease pathogenesis in the R6/2 mouse model of Huntington's disease. PLoS One 4(6):e5747.
51. Dai Y, Dudek NL, Li Q, Fowler SC, & Muma NA (2009) Striatal expression of a calmodulin fragment improved motor function, weight loss, and neuropathology in the R6/2 mouse model of Huntington's disease. J Neurosci 29(37):11550-11559.
52. Moncho-Bogani J, Martinez-Garcia F, Novejarque A, & Lanuza E (2005) Attraction to sexual pheromones and associated odorants in female mice involves activation of the reward system and basolateral amygdala. Eur J Neurosci 21(8):2186-2198.
53. Oorschot DE (1996) Total number of neurons in the neostriatal, pallidal, subthalamic, and substantia nigral nuclei of the rat basal ganglia: a stereological study using the cavalieri and optical disector methods. J Comp Neurol 366(4):580-599.

Figure Legends

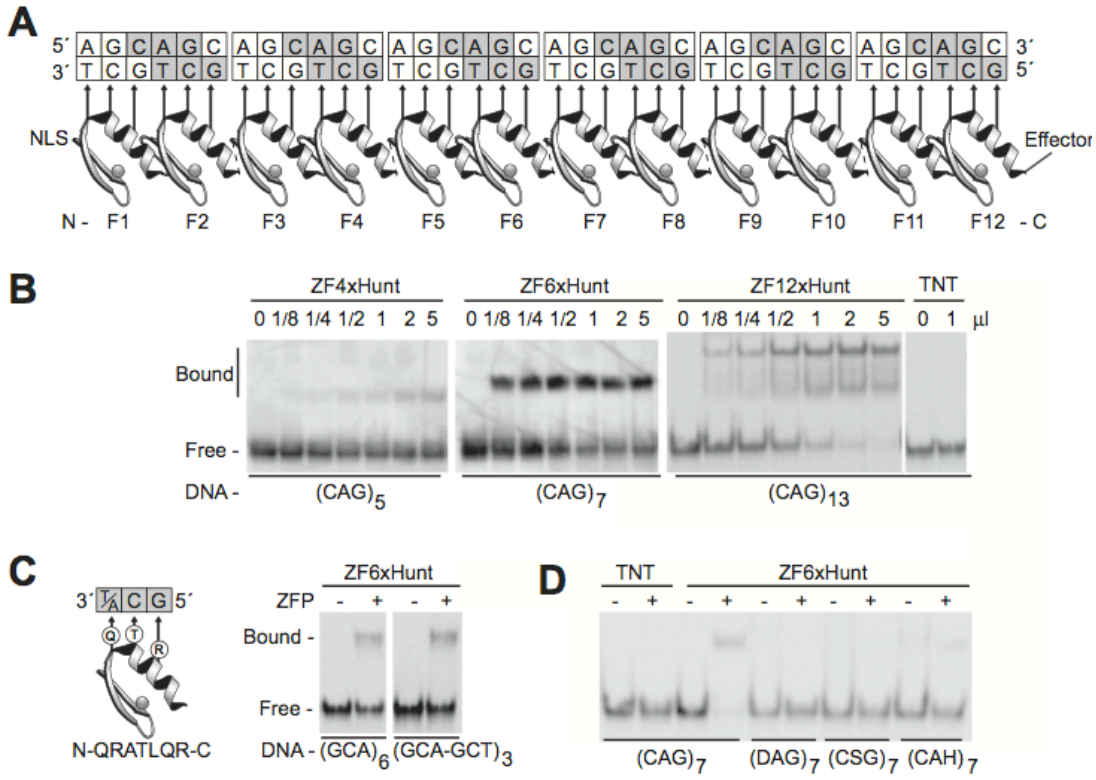

Figure 1. Zinc finger arrays to bind CAG-repeats. (A) A 12-finger array, showing recognition helices contacting 5'-GCT-3' bases on the lower DNA strand. Similar arrays of 4, 6, 12 or 18 zinc fingers were built (ZF4xHunt, ZF6xHunt, ZF12xHunt and ZF18xHunt). Nuclear localization signals (NLS) and effectors (e.g. Kox-1 transcription repression domain) were added to N- and C- termini, respectively. (B) Gel shift assays show 4-, 6- or 12-finger arrays binding poly-CAG DNA and forming distinct complexes. Negative control: transcription-translation mix (TNT). (C) The hybrid zinc finger design recognizes 5'-GC(A/T)-3', allowing binding to either the $(GCA)_n$ or the $(GCT)_n$ complementary strands of the CAG-repeat. A gel shift assay shows equal binding to GCA or GCT triplets in mixed sequences. (D) Specificity gel shift assay. Zinc fingers bind preferentially to CAG repeats (CAG_7) when compared to degenerate mutant sequences (DAG_7, CSG_7 or CAH_7; D=A,G,T; S=C,G; H=A,C,T).

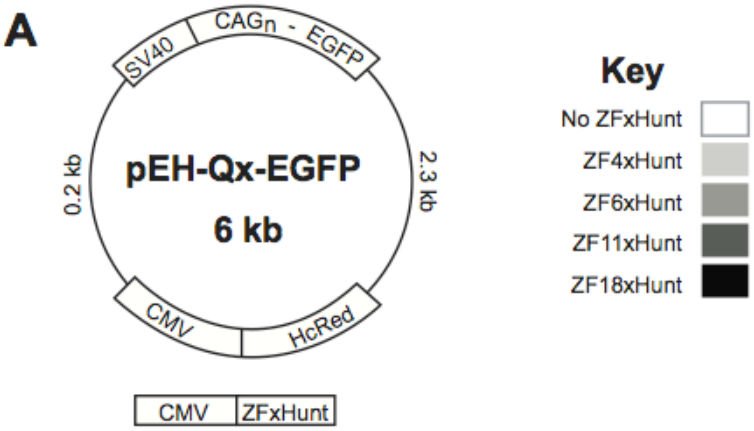
A
SV40
CAGn - EGFP
pEH-Qx-EGFP
6 kb
0.2 kb
2.3 kb
CMV
HcRed
CMV
ZFxHunt
Key
No ZFxHunt
ZF4xHunt
ZF6xHunt
ZF11xHunt
ZF18xHunt

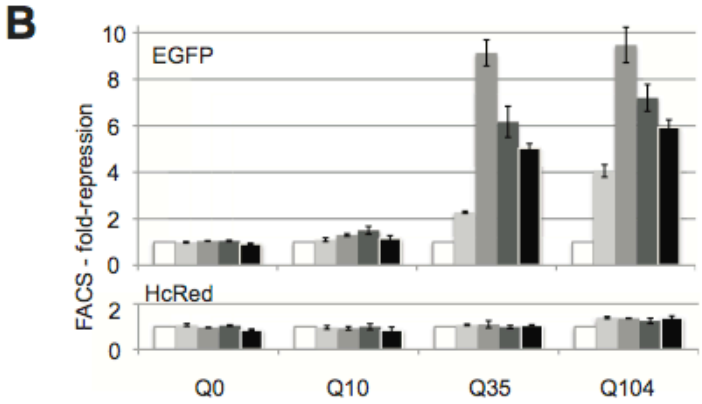
B
EGFP
FACS - fold-repression
10
8
6
4
2
0
HcRed
2
0
Q0
Q10
Q35
Q104

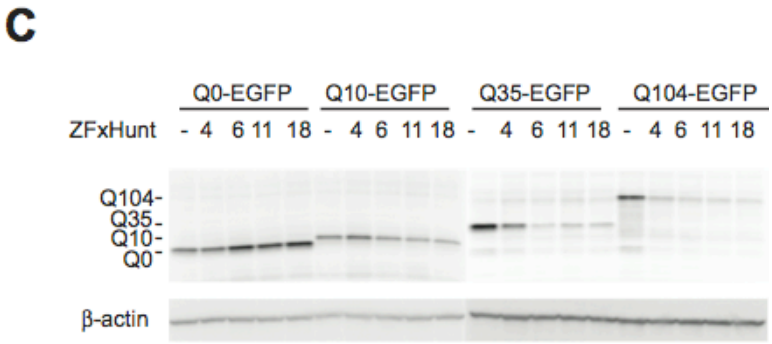
C
Q0-EGFP
Q10-EGFP
Q35-EGFP
Q104-EGFP
ZFxHunt - 4 6 11 18 - 4 6 11 18 - 4 6 11 18 - 4 6 11 18
Q104-
Q35-
Q10-
Q0-
β-actin

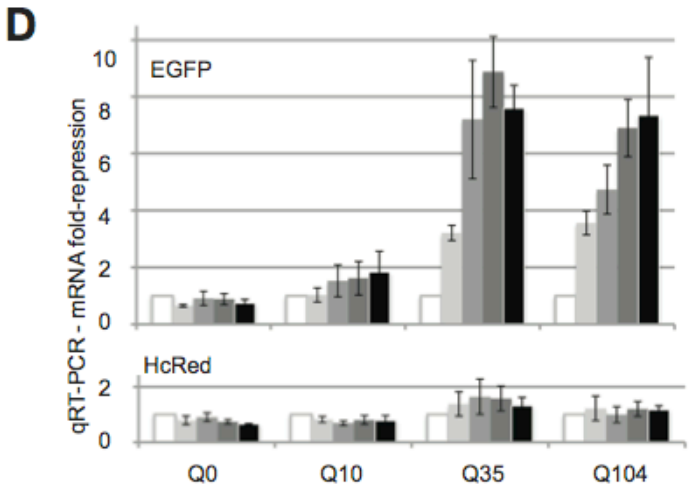
D
EGFP
qRT-PCR - mRNA fold-repression
10
8
6
4
2
0
HcRed
2
0
Q0
Q10
Q35
Q104

Figure 2. Episomal poly-CAG-reporter repression by ZFxHunt. (A) The pEH reporter plasmid contains EGFP, fused to the N-terminal CAG repeats of the human *HTT* gene, expressing different-length poly-Q coding sequences under an SV40 promoter. A control HcRed gene, under a CMV promoter, measures off-target or long-range repression. Key: ZFP expression constructs (0 - 18 fingers). (B) FACS assay measuring the fold-reduction in EGFP and HcRED fluorescent cells, in response to different zinc fingers. A 10-fold repression is equivalent to 90% reduction. Results are the mean +/- s.e.m of three independent experiments. (C) EGFP Western blot for ZFP repression of pEH-Qx targets. (D) qRT-PCR assay to measure fold-repression of EGFP or HcRED mRNA by ZFP. Results are the mean +/- s.e.m of four independent experiments.

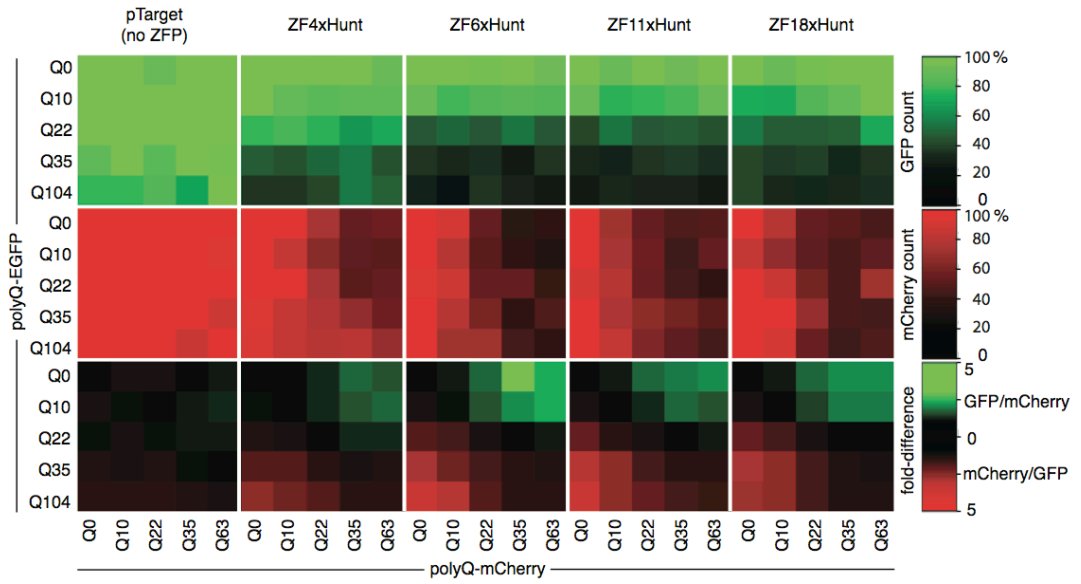

Figure 3. ZFP competition assay against pairs of different-length CAG repeats. Each small square represents one transfection experiment, where cells simultaneously receive two reporter plasmids: poly-Q-EGFP and poly-Q-mCherry of different lengths (Q0 to Q104). ZFxHunt with 4-, 6-, 11- or 18-fingers were tested for their ability to reduce the number of detectable green and red cells in FACS assays (%). Longer poly-Q constructs are repressed preferentially, resulting in the shorter green or shorter red poly-Q constructs dominating expression.

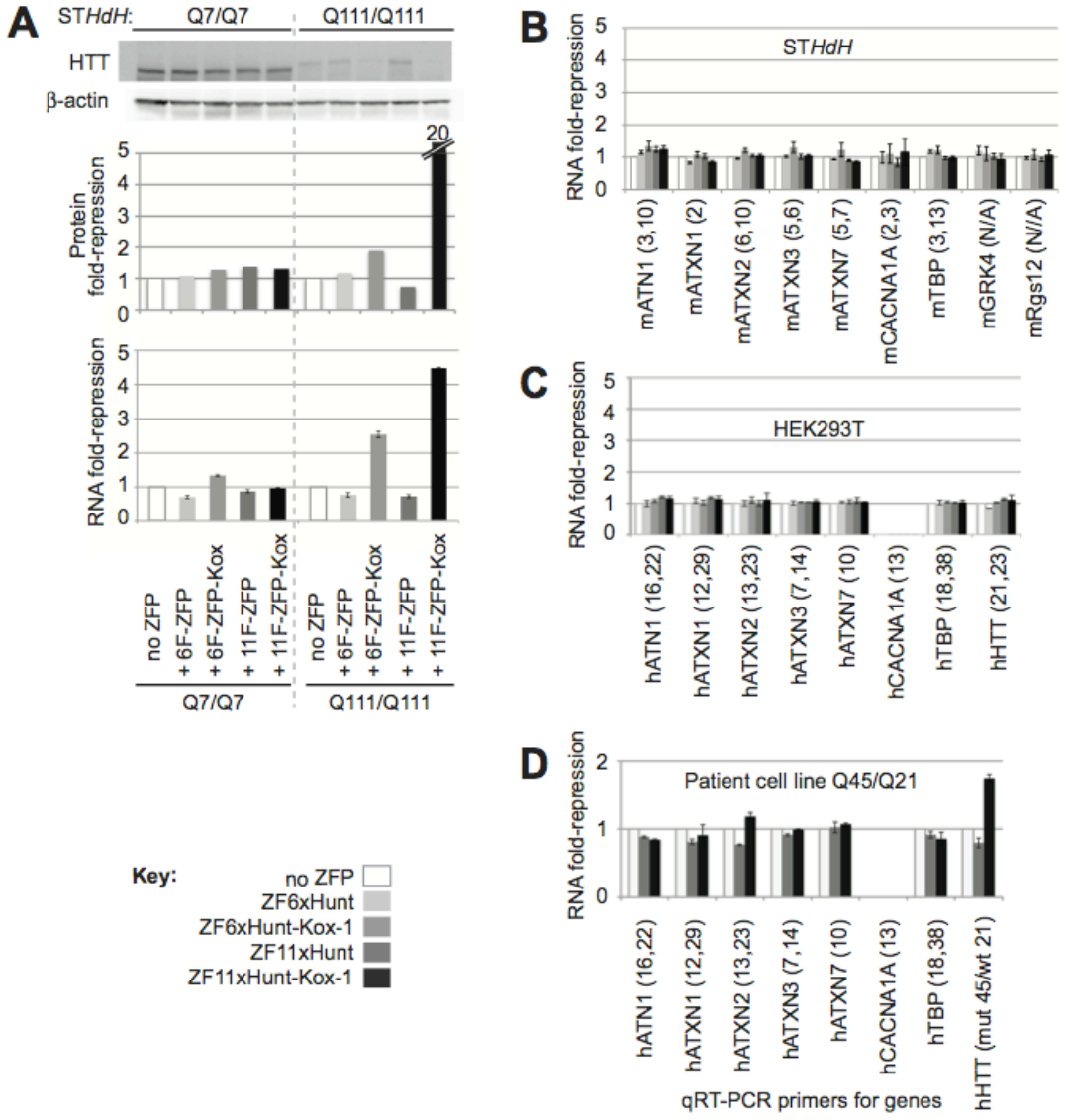

Figure 4. Expression of chromosomal CAG-repeat genes, 20 days after retroviral ZFP delivery. Assays were carried out in wt mouse ST*Hdh* cells (Q7/Q7), in poly-Q ST*Hdh* mutants (Q111/Q111), and in human HEK293T, as indicated. Mouse and human genes are prefixed by "m" and "h", respectively. (A) Repression of endogenous *HTT* by ZF6xHunt and ZF11xHunt, with and without Kox-1 repressor domain. Western blots for HTT (top) were controlled with β-actin staining and quantified using ImageJ (Protein fold-repression; middle). qRT-PCR was used to compare *HTT* mRNA levels (RNA fold repression; bottom). The experiment was repeated independently three times with similar results; one experiment is displayed. (B) The mRNA levels of other wt CAG-repeat genes are broadly unaffected in ST*Hdh* cells (pooled samples: 3 Q7/Q7 and 3 Q111/Q111). 7 genes were tested by qRT-PCR (atrophin1: ATN1; ataxin-1-3,7: ATXN1-3,7; calcium channel alpha 1A subunit:

CACNA1A; TATA binding protein: TBP). CAG-repeat numbers are in brackets; The first number corresponds to pure CAG repeats, the second number to broken CAG repeats (containing CAA or CAT). Two genomic neighbours of *HTT*, (G protein-coupled receptor kinase 4: GRK4, ~7 kb upstream; G-protein signaling 12: Rgs12, ~188 kb downstream) were also unaffected in ST*Hdh* cells. (C) The mRNA levels of the 7 wt human CAG genes and *HTT* (huntingtin; 21 repeats) were also broadly unaffected in HEK293T cells. (D) ZF11xHunt-Kox-1 represses only *HTT* in a heterozygous human patient-derived cell line (mut Q45/wt Q21). RNA was extracted from FACS-sorted transduced cells, 7 days after infection. N.B. CACNA1A is not expressed in HEK293T or the Q45/Q21 patient cell line.

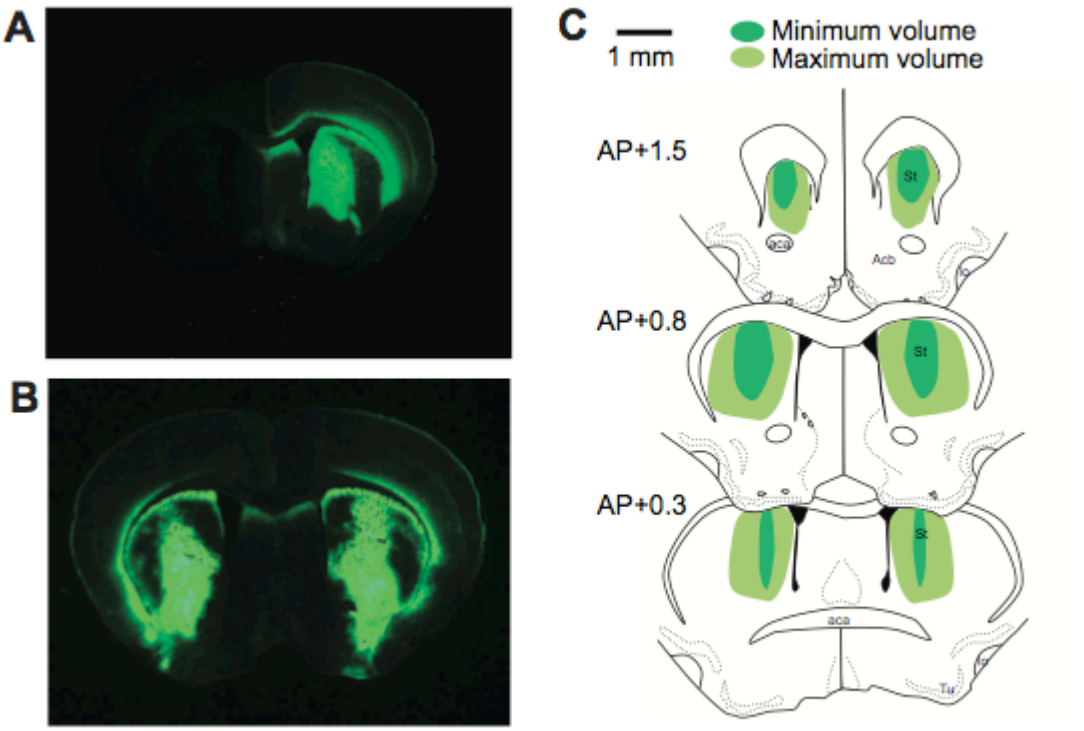

Figure 5. Gene delivery by stereotaxis. (A) A cross-section of mouse brain, injected in one hemisphere with AAV2/1-CAG-GFP-WPRE, reveals widespread green fluorescence in the striatum. (B) Similar distributions are seen when injecting the GFP construct in both hemispheres (as for the behavioural assay). The zinc finger construct AAV2/1-CAG-ZF11xHunt-Kox-1-WPRE was injected at identical titre, in one or both hemispheres, as described. (C) Schematic drawings showing the maximum and minimum volume covered by GFP expression in mice injected in both hemispheres (n=4). AP levels as in Paxinos and Watson atlas of the mouse brain. aca= anterior comissure; Acb=nucleus accumbens; lo=olfactory tract; St=striatum; Tu=olfactory tubercle.

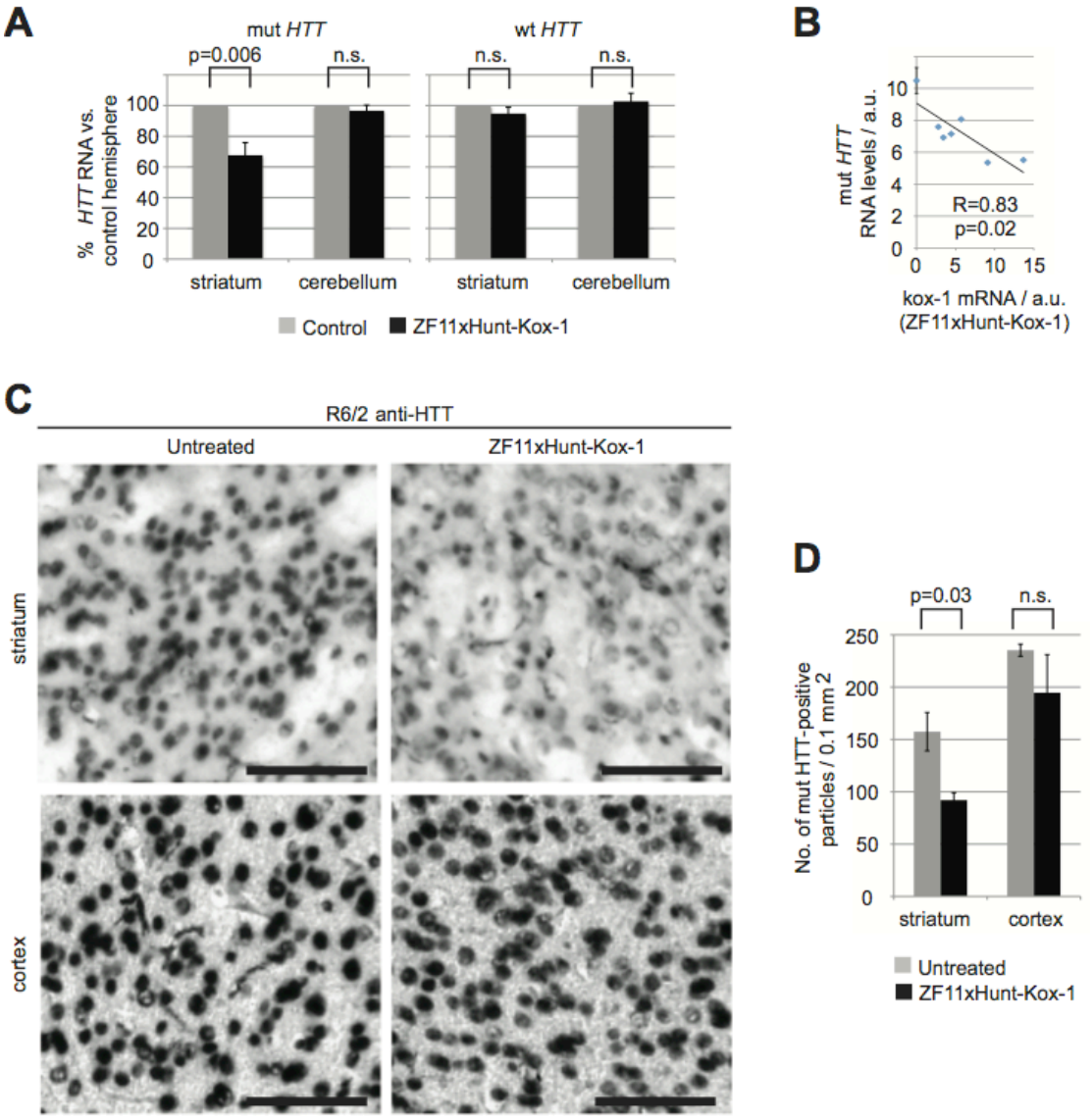

Figure 6. ZF repression *in vivo* (A) qRT-PCR data quantifying mRNA levels in mouse samples injected striatally with ZF11xHunt-Kox-1, compared to the control hemisphere. Mutant *HTT* (mut *HTT*) is repressed ~40% by the zinc finger construct in the striatum, whereas it is unaffected in the non-injected cerebellum. Wild-type *HTT* (wt *HTT*) is unaffected in all samples. Mut *HTT* n=6; wt *HTT* n=9. Control groups contain both untreated and GFP-treated mice (the groups are similar; Fig. S6B). (B) Linear regression analysis of zinc finger expression (ZF11xHunt-Kox-1) versus mut *HTT* expression shows a significant negative correlation (p=0.02)**.** Data are from the treated hemispheres (n=6) and the corresponding untreated hemispheres (mean +/- s.e.m.). (C) Anti-HTT immunostaining of brain samples reveals a reduction of mutant aggregates in injected striatum with ZF11xHunt-Kox-1 treatment. Scale bars: 100 μm. (D) Quantifying HTT-positive aggregates by automatic counting of mut HTT positive particles with ImageJ software, as previously described (52)(Fig. S7). The data are

from 3 mice and represent comparisons between their injected and non-injected hemispheres, in striatum and cortex.

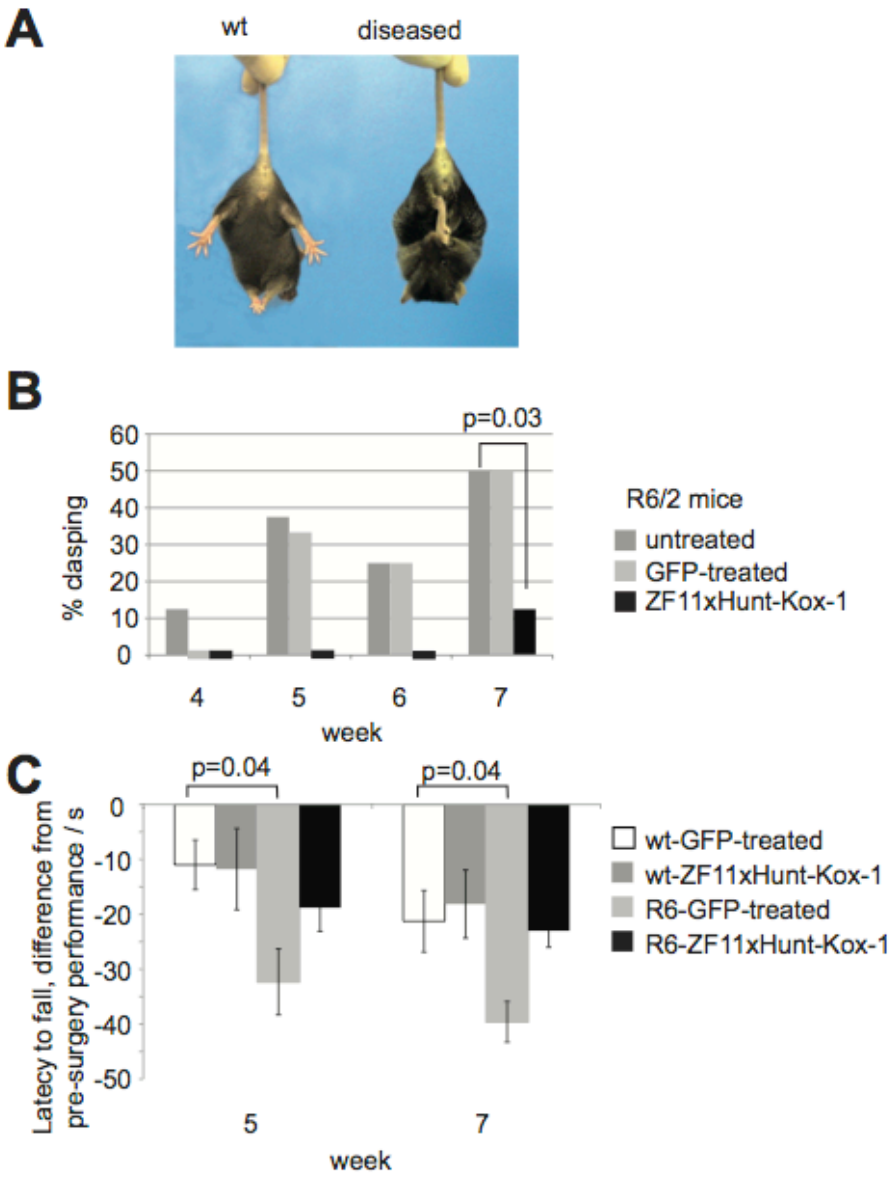

Figure 7. Rescue of HD phenotypes with *in vivo* ZF treatment. (A) HD mice show a characteristic clasping behaviour (diseased) corresponding to neurological pathology (43). (B) The clasping assay shows a significant improvement after zinc finger treatment in both hemispheres (p=0.03). Only 1 in 8 ZF-treated mice display symptoms by week 7, compared with 6 in 12 control mice. (C) Performance in the accelerating rotarod shows a clear decline with respect to pre-surgery levels in the GFP-injected R6/2 mice, whereas ZF-treated mice do not show a significant decline as compared to WT mice.

Supplementary Information

Synthetic zinc finger repressors reduce mutant *HTT* expression in the brain of R6/2 mice.

Mireia Garriga-Canut, Carmen Agustín-Pavón, Frank Herrmann, Mara Dierssen,

Cristina Fillat and Mark Isalan

EMBL/CRG Systems Biology Research Unit, Centre for Genomic Regulation (CRG), UPF, 08003 Barcelona, Spain.

Table of contents

The DNA and protein sequences of ZF6xHunt-Kox-1 and ZF12xHunt-Kox-1

The following coding sequences were cloned into the pTarget plasmid (Promega), to include a CMV promoter (followed by an intron and part of lacZ).

Key

ATG=start codon
3XFLAG-TAG
NLS: nuclear localisation signal
Zinc finger sequence, α-helices underlined in protein
linker sequences in bold in protein
Kox-1 repressor domain
TAA=stop codon

>ZF6xHunt-Kox-1_DNA

ATGGCCGACTACAAAGACCATGACGGTGATTATAAAGATCATGACATCGACTACAAA
GACGATGACGACAAGCCGAAGAAAAAACGTAAAGTGACCGGGGCCGAGCGCCCCTTC
CAGTGCCGCATTTGTATGCGCAACTTTAGCCAGCGCGCGACCCTGCAGCGTCATATT
CGCACCCATACCGGTGAAAAACCGTTTGCGTGCGATATTTGCGGTCGTAAATTTGCG
CAGCGTGCGACCCTGCAGCGCCATACCAAAATTCACACCGGATCCGAACGGCCGTTT
CAGTGCCGTATTTGCATGCGTAATTTTAGCCAGCGTGCGACCCTGCAGCGCCATATT
CGTACCCATACCGGTGAAAAACCGTTTGCCTGCGATATTTGTGGCCGTAAATTTGCC
CAGCGCGCGACCCTGCAGCGCCATACCAAAATTCATACCGGTTCTGAACGGCCGTTT
CAGTGCAGGATTTGCATGCGTAATTTTTCCCAGCGCGCGACCCTGCAGCGCCATATT
CGCACCCATACTGGTGAAAAACCGTTTGCCTGCGATATTTGCGGTCGTAAATTTGCG
CAGCGTGCTACCTTACAGCGCCATACCAAAATTCATCTGCGCCAGAAAGATGGTGGC
GGCGGCTCAGGTGGCGGCGGTAGTGGTGGCGGCGGCTCACAACTAGTCTCTAGTTTG
TCTCCTCAGCACTCTGCTGTCACTCAAGGAAGTATCATCAAGAACAAGGAGGGCATG
GATGCTAAGTCACTAACTGCCTGGTCCCGGACACTGGTGACCTTCAAGGATGTATTT
GTGGACTTCACCAGGGAGGAGTGGAAGCTGCTGGACACTGCTCAGCAGATCGTGTAC
AGAAATGTGATGCTGGAGAACTATAAGAACCTGGTTTCCTTGGGTTATCAGCTTACT
AAGCCAGATGTGATCCTCCGGTTGGAGAAGGGAGAAGAGCCCTGGCTGGTGGAGAGA
GAAATTCACCAAGAGACCCATCCTGATTCAGAGACTGCATTTGAAATCAAATCATCA
GTTTAA

>ZF6xHunt-Kox-1_protein

MADYKDHDGDYKDHDIDYKDDDDK **PKKKRKV** **TGAERP**
FQCRICMRNFSQRATLQRHIRTH **TGEKP**
FACDICGRKFAQRATLQRHTKIH **TGSERP**
FQCRICMRNFSQRATLQRHIRTH **TGEKP**
FACDICGRKFAQRATLQRHTKIH **TGSERP**
FQCRICMRNFSQRATLQRHIRTH **TGEKP**
FACDICGRKFAQRATLQRHTKIH **LRQKDGGGGSGGGGSGGGGSQLV**
SSLSPQHSAVTQGSIIKNKEGMDAKSLTAWSRTLVTFKDVFVDFTREEWKLLDTAQQ
IVYRNVMLENYKNLVSLGYQLTKPDVILRLEKGEEPWLVEREIHQETHPDSETAFEI
KSSV*

>ZF11xHunt-KoxI_DNA

ATGGCCgactacaaagaccatgacggtgattataaagatcatgacatcgactacaaa
gacgatgacgacaagCCGAAGAAAAAACGTAAAGTGACCGGGGCCGAGCGCCCCTTC
CAGTGCCGCATTTGTATGCGCAACTTTAGCCAGCGCGCGACCCTGCAGCGCCATACC
AAAATTCACACCGGATCCGAACGGCCGTTTCAGTGCCGTATTTGCATGCGTAATTTT
AGCCAGCGTGCGACCCTGCAGCGCCATATTCGTACCCATACCGGTGAAAAACCGTTT
GCCTGCGATATTTGTGGCCGTAAATTTGCCCAGCGCGCGACCCTGCAGCGCCATACC
AAAATTCATACCGGTTCTGAACGGCCGTTTCAGTGCAGGATTTGCATGCGTAATTTT
TCCCAGCGCGCGACCCTGCAGCGCCATATTCGCACCCATACTGGTGAAAAACCGTTT
GCCTGCGATATTTGCGGTCGTAAATTTGCGCAGCGTGCTACCTTACAGCGCCATACC
AAAATTCATCTGCGCCAGAAAGATGGTGGCGGCGGCTCAGGTGGCGGCGGTAGTGGT
GGCGGCGGCTCACAACTAGTCGGTACCGCCGAGCGCCCCTTCCAGTGCCGCATTTGT
ATGCGCAACTTTAGCCAGCGCGCGACCCTGCAGCGTCATATTCGCACCCATACCGGT
GAAAAACCGTTTGCGTGCGATATTTGCGGTCGTAAATTTGCGCAGCGTGCGACCCTG
CAGCGCCATACCAAAATTCACACCGGATCCGAACGGCCGTTTCAGTGCCGTATTTGC
ATGCGTAATTTTAGCCAGCGTGCGACCCTGCAGCGCCATATTCGTACCCATACCGGT
GAAAAACCGTTTGCCTGCGATATTTGTGGCCGTAAATTTGCCCAGCGCGCGACCCTG
CAGCGCCATACCAAAATTCATACCGGTTCTGAACGGCCGTTTCAGTGCAGGATTTGC
ATGCGTAATTTTTCCCAGCGCGCGACCCTGCAGCGCCATATTCGCACCCATACTGGT
GAAAAACCGTTTGCCTGCGATATTTGCGGTCGTAAATTTGCGCAGCGTGCTACCTTA
CAGCGCCATACCAAAATTCATCTGCGCCAGAAAGATGGTGGCGGCGGCTCAGGTGGC
GGCGGTAGTGGTGGCGGCGGCTCACAACTAGTCTCTAGtttgtctcctcagcactct
gctgtcactcaaggaagtatcatcaagaacaaggagggcatggatgctaagtcacta
actgcctggtcccggacactggtgaccttcaaggatgtatttgtggacttcaccagg
gaggagtggaagctgctggacactgctcagcagatcgtgtacagaaatgtgatgctg
gagaactataagaacctggtttccttgggttatcagcttactaagccagatgtgatc
ctccggttggagaagggagaagagccctggctggtggagagagaaattcaccaagag
acccatcctgattcagagactgcatttgaaatcaaatcatcagttTAA

>ZF11xHunt-KoxI_protein

MADYKDHDGDYKDHDIDYKDDDDK PKKKRKV TGAERP
FQCRICMRNFSQRATLQRHTKIH TGSERP
FQCRICMRNFSQRATLQRHIRTH TGEKP
FACDICGRKFAQRATLQRHTKIH TGSERP
FQCRICMRNFSQRATLQRHIRTH TGEKP
FACDICGRKFAQRATLQRHTKIH LRQKDGGGGSGGGGSGGGGSQLVGTAERP
FQCRICMRNFSQRATLQRHIRTH TGEKP
FACDICGRKFAQRATLQRHTKIH TGSERP
FQCRICMRNFSQRATLQRHIRTH TGEKP
FACDICGRKFAQRATLQRHTKIH TGSERP
FQCRICMRNFSQRATLQRHIRTH TGEKP
FACDICGRKFAQRATLQRHTKIH LRQKDGGGGSGGGGSGGGGSQLV
SSLSPQHSAVTQGSIIKNKEGMDAKSLTAWSRTLVTFKDVFVDFTREEWKLLDTAQQ
IVYRNVMLENYKNLVSLGYQLTKPDVILRLEKGEEPWLVEREIHQETHPDSE
TAFEIKSSV*

>ZF12xHunt-DNA (no Kox-1)

ATGGCCGACTACAAAGACCATGACGGTGATTATAAAGATCATGACATCGACTACAAA
GACGATGACGACAAGCCGAAGAAAAAACGTAAAGTGACCGGGGCCGAGCGCCCCTTC
CAGTGCCGCATTTGTATGCGCAACTTTAGCCAGCGCGCGACCCTGCAGCGTCATATT
CGCACCCATACCGGTGAAAAACCGTTTGCGTGCGATATTTGCGGTCGTAAATTTGCG
CAGCGTGCGACCCTGCAGCGCCATACCAAAATTCACACCGGATCCGAACGGCCGTTT
CAGTGCCGTATTTGCATGCGTAATTTTAGCCAGCGTGCGACCCTGCAGCGCCATATT
CGTACCCATACCGGTGAAAAACCGTTTGCCTGCGATATTTGTGGCCGTAAATTTGCC
CAGCGCGCGACCCTGCAGCGCCATACCAAAATTCATACCGGTTCTGAACGGCCGTTT
CAGTGCAGGATTTGCATGCGTAATTTTTCCCAGCGCGCGACCCTGCAGCGCCATATT
CGCACCCATACTGGTGAAAAACCGTTTGCCTGCGATATTTGCGGTCGTAAATTTGCG
CAGCGTGCTACCTTACAGCGCCATACCAAAATTCATCTGCGCCAGAAAGATGGTGGC
GGCGGCTCAGGTGGCGGCGGTAGTGGTGGCGGCGGCTCACAACTAGTCGGTACCGCC
GAGCGCCCCTTCCAGTGCCGCATTTGTATGCGCAACTTTAGCCAGCGCGCGACCCTG
CAGCGTCATATTCGCACCCATACCGGTGAAAAACCGTTTGCGTGCGATATTTGCGGT
CGTAAATTTGCGCAGCGTGCGACCCTGCAGCGCCATACCAAAATTCACACCGGATCC
GAACGGCCGTTTCAGTGCCGTATTTGCATGCGTAATTTTAGCCAGCGTGCGACCCTG
CAGCGCCATATTCGTACCCATACCGGTGAAAAACCGTTTGCCTGCGATATTTGTGGC
CGTAAATTTGCCCAGCGCGCGACCCTGCAGCGCCATACCAAAATTCATACCGGTTCT
GAACGGCCGTTTCAGTGCAGGATTTGCATGCGTAATTTTTCCCAGCGCGCGACCCTG
CAGCGCCATATTCGCACCCATACTGGTGAAAAACCGTTTGCCTGCGATATTTGCGGT
CGTAAATTTGCGCAGCGTGCTACCTTACAGCGCCATACCAAAATTCATCTGCGCCAG
AAAGATGGTGGCGGCGGCTCAGGTGGCGGCGGTAGTGGTGGCGGCGGCTCACAACTA
GTCTAA

>ZF12xHunt-Protein (no Kox-1)

MADYKDHDGDYKDHDIDYKDDDDK **PKKKRKV** **TGAERP**
FQCRICMRNFSQRATLQRHIRTH **TGEKP**
FACDICGRKFAQRATLQRHTKIH **TGSERP**
FQCRICMRNFSQRATLQRHIRTH **TGEKP**
FACDICGRKFAQRATLQRHTKIH **TGSERP**
FQCRICMRNFSQRATLQRHIRTH **TGEKP**
FACDICGRKFAQRATLQRHTKIH **LRQKDGGGGSGGGGSGGGGSQLVGTAERP**
FQCRICMRNFSQRATLQRHIRTH **TGEKP**
FACDICGRKFAQRATLQRHTKIH **TGSERP**
FQCRICMRNFSQRATLQRHIRTH **TGEKP**
FACDICGRKFAQRATLQRHTKIH **TGSERP**
FQCRICMRNFSQRATLQRHIRTH **TGEKP**
FACDICGRKFAQRATLQRHTKIH **LRQKDGGGGSGGGGSGGGGSQLV***

>ZF18xHunt-DNA (no Kox-1)

ATGGCCGACTACAAAGACCATGACGGTGATTATAAAGATCATGACATCGACTACAAAGACGATGACGAC
AAGCCGAAGAAAAAACGTAAAGTGACCGGGGCCGAGCGCCCCTTCCAGTGCCGCATTTGTATGCGCAAC
TTTAGCCAGCGCGCGACCCTGCAGCGTCATATTCGCACCCATACCGGTGAAAAACCGTTTGCGTGCGAT
ATTTGCGGTCGTAAATTTGCGCAGCGTGCGACCCTGCAGCGCCATACCAAAATTCACACCGGATCCGAA
CGGCCGTTTCAGTGCCGTATTTGCATGCGTAATTTTAGCCAGCGTGCGACCCTGCAGCGCCATATTCGT
ACCCATACCGGTGAAAAACCGTTTGCCTGCGATATTTGTGGCCGTAAATTTGCCCAGCGCGCGACCCTG
CAGCGCCATACCAAAATTCATACCGGTTCTGAACGGCCGTTTCAGTGCAGGATTTGCATGCGTAATTTT
TCCCAGCGCGCGACCCTGCAGCGCCATATTCGCACCCATACTGGTGAAAAACCGTTTGCCTGCGATATT
TGCGGTCGTAAATTTGCGCAGCGTGCTACCTTACAGCGCCATACCAAAATTCATCTGCGCCAGAAAGAT
GGTGGCGGCGGCTCAGGTGGCGGCGGTAGTGGTGGCGGCGGCTCACAACTAGTCGGTACCGCCGAGCGC
CCCTTCCAGTGCCGCATTTGTATGCGCAACTTTAGCCAGCGCGCGACCCTGCAGCGTCATATTCGCACC
CATACCGGTGAAAAACCGTTTGCGTGCGATATTTGCGGTCGTAAATTTGCGCAGCGTGCGACCCTGCAG
CGCCATACCAAAATTCACACCGGATCCGAACGGCCGTTTCAGTGCCGTATTTGCATGCGTAATTTTAGC
CAGCGTGCGACCCTGCAGCGCCATATTCGTACCCATACCGGTGAAAAACCGTTTGCCTGCGATATTTGT
GGCCGTAAATTTGCCCAGCGCGCGACCCTGCAGCGCCATACCAAAATTCATACCGGTTCTGAACGGCCG
TTTCAGTGCAGGATTTGCATGCGTAATTTTTCCCAGCGCGCGACCCTGCAGCGCCATATTCGCACCCAT
ACTGGTGAAAAACCGTTTGCCTGCGATATTTGCGGTCGTAAATTTGCGCAGCGTGCTACCTTACAGCGC
CATACCAAAATTCATCTGCGCCAGAAAGATGGTGGCGGCGGCTCAGGTGGCGGCGGTAGTGGTGGCGGC
GGCTCACAACTAGTCGGTACCGCCGAGCGCCCCTTCCAGTGCCGCATTTGTATGCGCAACTTTAGCCAG
CGCGCGACCCTGCAGCGTCATATTCGCACCCATACCGGTGAAAAACCGTTTGCGTGCGATATTTGCGGT
CGTAAATTTGCGCAGCGTGCGACCCTGCAGCGCCATACCAAAATTCACACCGGATCCGAACGGCCGTTT
CAGTGCCGTATTTGCATGCGTAATTTTAGCCAGCGTGCGACCCTGCAGCGCCATATTCGTACCCATACC
GGTGAAAAACCGTTTGCCTGCGATATTTGTGGCCGTAAATTTGCCCAGCGCGCGACCCTGCAGCGCCAT
ACCAAAATTCATACCGGTTCTGAACGGCCGTTTCAGTGCAGGATTTGCATGCGTAATTTTTCCCAGCGC
GCGACCCTGCAGCGCCATATTCGCACCCATACTGGTGAAAAACCGTTTGCCTGCGATATTTGCGGTCGT
AAATTTGCGCAGCGTGCTACCTTACAGCGCCATACCAAAATTCATCTGCGCCAGAAAGATGGTGGCGGC
GGCTCAGGTGGCGGCGGTAGTGGTGGCGGCGGCTCACAACTAGTCTAA

>ZF12xHunt-Protein (no Kox-1)

MADYKDHDGDYKDHDIDYKDDDDK **PKKKRKV** **TGAERP**
FQCRICMRNFSQRATLQRHIRTH **TGEKP**
FACDICGRKFAQRATLQRHTKIH **TGSERP**
FQCRICMRNFSQRATLQRHIRTH **TGEKP**
FACDICGRKFAQRATLQRHTKIH **TGSERP**
FQCRICMRNFSQRATLQRHIRTH **TGEKP**
FACDICGRKFAQRATLQRHTKIH **LRQKDGGGGSGGGGSGGGGSQLVGTAERP**
FQCRICMRNFSQRATLQRHIRTH **TGEKP**
FACDICGRKFAQRATLQRHTKIH **TGSERP**
FQCRICMRNFSQRATLQRHIRTH **TGEKP**
FACDICGRKFAQRATLQRHTKIH **TGSERP**
FQCRICMRNFSQRATLQRHIRTH **TGEKP**
FACDICGRKFAQRATLQRHTKIH **LRQKDGGGGSGGGGSGGGGSQLVGTAERP**
FQCRICMRNFSQRATLQRHIRTH **TGEKP**
FACDICGRKFAQRATLQRHTKIH **TGSERP**
FQCRICMRNFSQRATLQRHIRTH **TGEKP**
FACDICGRKFAQRATLQRHTKIH **TGSERP**
FQCRICMRNFSQRATLQRHIRTH **TGEKP**
FACDICGRKFAQRATLQRHTKIH **LRQKDGGGGSGGGGSGGGGSQLV***

Supplementary Table S1. Students' t-test analysis of the fold repression data against an expected value of 1, from the FACS experiment in Fig. 2B.

ZF	Number of repeats	Reporter gene	p-value
ZF4xHunt	Q0	EGFP	0.894
	Q10		0.363
	Q35		<0.001
	Q104		<0.001
	Q0	HcRed	0.325
	Q10		0.706
	Q35		0.128
	Q104		0.004
ZF6xHunt	Q0	EGFP	0.010
	Q10		0.020
	Q35		<0.001
	Q104		<0.001
	Q0	HcRed	0.158
	Q10		0.468
	Q35		0.540
	Q104		<0.001
ZF11xHunt	Q0	EGFP	0.157
	Q10		0.046
	Q35		<0.001
	Q104		<0.001
	Q0	HcRed	0.221
	Q10		0.990
	Q35		0.848
	Q104		0.109
ZF18xHunt	Q0	EGFP	0.281
	Q10		0.280
	Q35		<0.001
	Q104		<0.001
	Q0	HcRed	0.090
	Q10		0.437
	Q35		0.077
	Q104		0.023

Supplementary Table S2. Students' t-test analysis of the fold repression data against an expected value of 1, from the qRT-PCR experiment in Fig. 2D.

ZF	Number of repeats	Reporter genes	p-value
ZF4xHunt	Q0	EGFP	0.005
	Q10		0.915
	Q35		0.004
	Q104		0.009
	Q0	HcRed	0.282
	Q10		0.207
	Q35		0.444
	Q104		0.644
ZF6xHunt	Q0	EGFP	0.735
	Q10		0.417
	Q35		0.059
	Q104		0.022
	Q0	HcRed	0.575
	Q10		0.038
	Q35		0.386
	Q104		0.994
ZF11xHunt	Q0	EGFP	0.582
	Q10		0.372
	Q35		0.008
	Q104		0.010
	Q0	HcRed	0.046
	Q10		0.318
	Q35		0.282
	Q104		0.495
ZF18xHunt	Q0	EGFP	0.145
	Q10		0.340
	Q35		0.004
	Q104		0.053
	Q0	HcRed	<0.001
	Q10		0.324
	Q35		0.349
	Q104		0.356

Table S3.
CAG-repeat number per gene and corresponding primer sets for qRT-PCR. Name prefixes: h=human; m=mouse. Approximate CAG repeat number for wild-type genes was obtained from Genbank mRNA data. CAG-repeat length: the first number corresponds to pure CAG repeats, the second number to broken CAG repeats (containing CAA or CAT).

Gene	CAG repeat length	Forward primer	Reverse primer
EGFP	0 - 104	CCTGAAGTTCATCTGCACCA	AAGTCGTGCTGCTTCATGTG
HcRed	0	AGATGCTGCGGAAGAAGAAG	GGTACCGTCGACTGCAGAA
hHPRT	N/A	CTTTGCTTTCCTTGGTCAGG	TATCCAACACTTCGTGGGGT
hATN1	16,22	GTCTCCCTCCGATCTGGATA	CACACTTCCAGGGCTGTAGA
hATXN1	12,29	CCAGCACCGTAGAGAGGATT	AGCCCTGTCCAAACACAAA
hATXN2	13,23	GACGCAGCTGAGCAAGTTAG	GAAGGAACGTGGGTTGAACT
hATXN3	7,14	AGAGCTTCGGAAGAGACGAG	ACTCCCAAGTGCTCCTGAAC
hATXN7	10	AACTGTGTGGCTCACTCTGG	TGGGAAGATGTTACCGTTGA
hCACNA1A	13	GGGAACTACACCCTCCTGAA	CGCTGCTTCTTCTTCCTCTT
hTBP	18,38	ACGCCGAATATAATCCCAAG	CTTCACTCTTGGCTCCTGTG
hHtt	21,23	CAGATGTCAGAATGGTGGCT	GCCTTGGAAGATTAGAATCCA
mATN1	3,10	CACCTGCCTCCACCTCATGGC	ATGCTCCTTGGGGGCCCTGG
mATXN1	2	TGTGGAGAGAATCGAGGAGA	CAGCCCTGTCCAAATACAAA
mATXN2	6,10	ATCCCAATGCAAAGGAGTTC	CTGCTGATGACCCACCATAG
mATXN3	5,6	ACCTCGCACTATTCTTGGCT	TGCATCTGTTGGACCTTGAT
mATXN7	5,7	TGCCCGTGTTCCTCACCGGA	GCGCGGAGACAGTGGTTGCT
mCACNA1A	2,3	CACTGGCAATAGCAAAGGAA	TTCTTGAGCGAGTTCACCAC
mTBP	3,13	ACTTCGTGCAAGAAATGCTG	GCTCATAGCTCTTGGCTCCT
mGRK4	N/A	TCCTGGCTTTGAGGAGCCGA	CCACAGCACAGCTCTGCAGCAT
mRgs12	N/A	GGGGGCTCAAGCAGGCATGG	GGGAGCCAGCCTCCGAGTCA
mHtt	4,7	CAGATGTCAGAATGGTGGCT	GCCTTGGAAGATTAGAATCCA
mHPRT	N/A	GGTTAAGCAGTACAGCCCCA	AGAGGTCCTTTTCACCAGCA
mActb	N/A	GCTTCTTTGCAGCTCCTTCGT	CCAGCGCAGCGATATCG
mAtp5b	N/A	CCACCGACATGGGCACAATGCA	ATGGGCAAAGGTGGTTGCAGGG

Table S4. Striatal volume and cell density are not affected by the genotype of mice or the treatment applied to the hemisphere (Repeated measures ANOVA, Genotype $p>0.1$; Treatment $p>0.1$ for both measures). Mean±SEM.

	Striatal volume (mm^3)		Cell density in the striatum (number of neuronal nuclei/mm^3)	
Genotype	Control	ZF11xHunt-Kox-1-Treated	Control	ZF11xHunt-Kox-1-Treated
WT	4.75±0.21	5.08±0.14	1116.23±90.14	991.92±110.71
R6/2	4.75±0.33	5.25±0.39	934.92±197.34	985.47±53.26

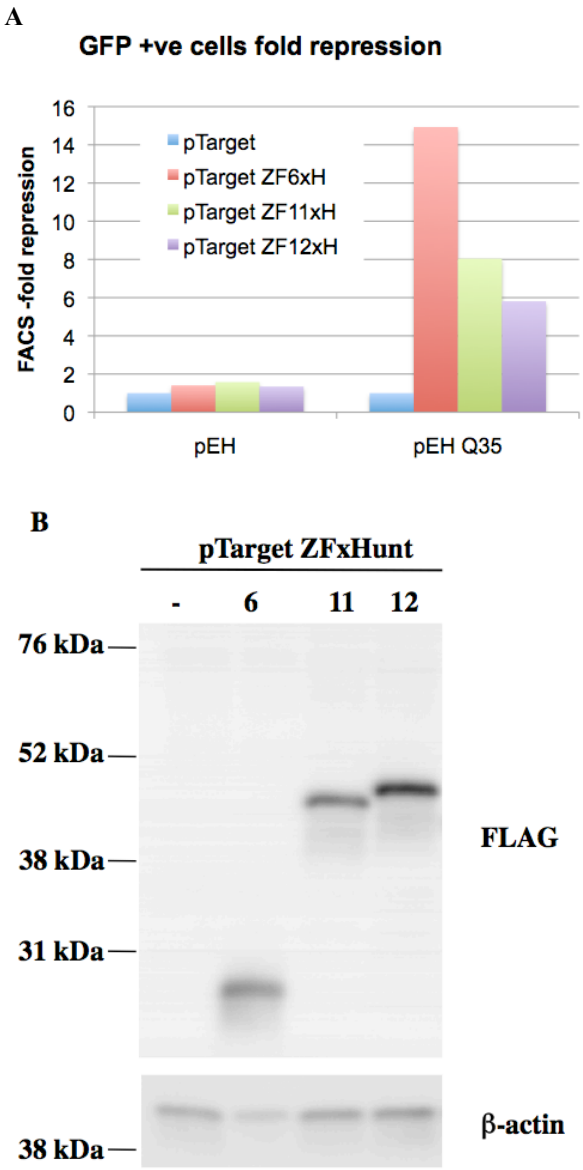

Figure S1. Comparison of ZF11xHunt and ZF12xHunt in episomal reporter repression. Cells were cotransfected with reporter and zinc finger plasmids: the pEH reporter plasmid contains EGFP, fused to Q35, under an SV40 promoter. pCMV-ZFxHunt (CMV promoter) expression constructs contain "naked" chains of ZFxHunt (6, 11 or 12 fingers, as indicated). The pTarget vector does not contain ZFP and is used as a control. FACS assay measuring the fold-reduction in EGFP fluorescent cells, in response to different "naked" zinc fingers **(A)**. A 5-fold repression is equivalent to 80% reduction. **(B)** FLAG Western blot for ZFP expression shows similar stability and expression levels for all constructs. β-actin staining is used as a loading control.

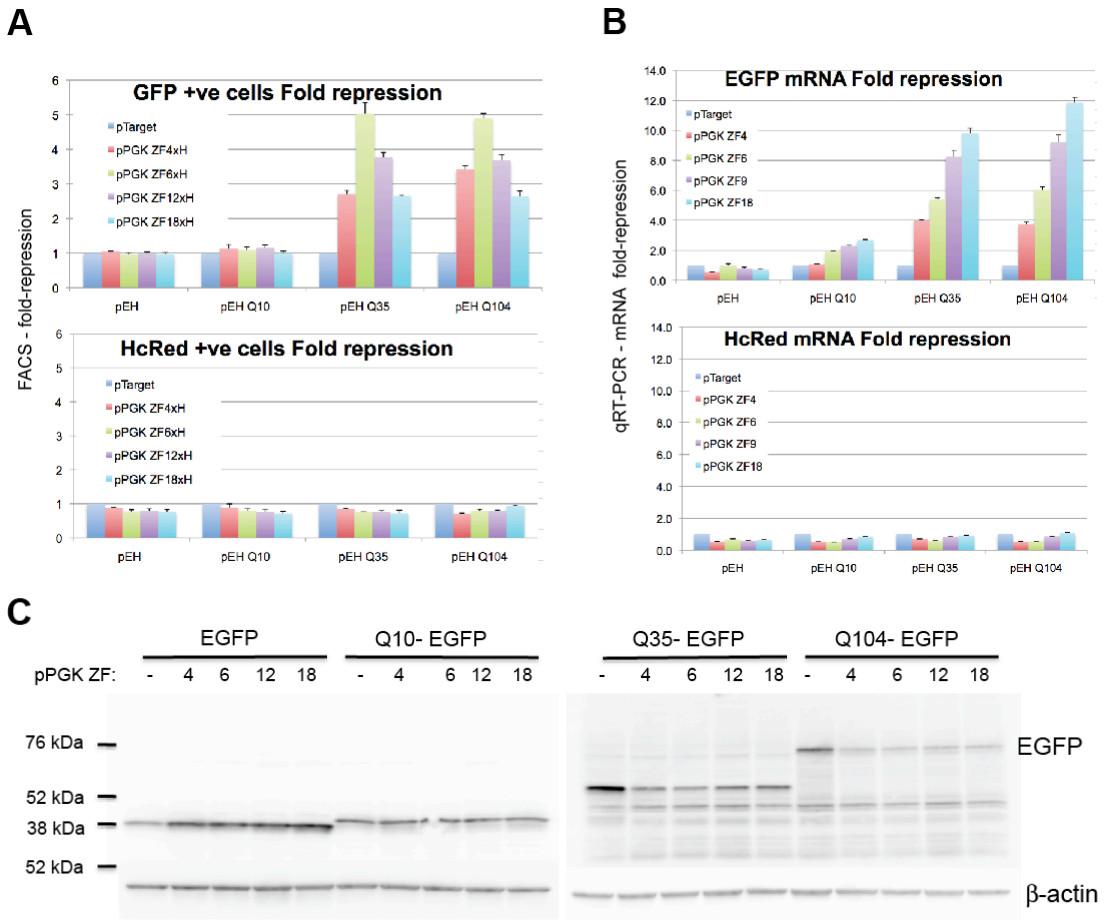

Figure S2. Episomal reporter repression by pPGK-ZFxHunt. Cells were cotransfected with reporter and zinc finger plasmids: the pEH reporter plasmid contains EGFP, fused to different-length poly-Q coding sequences, under an SV40 promoter. A control HcRed gene, under a CMV promoter, measures off-target or long-range repression. pPGK-ZF (PGK-promoter) expression constructs contain chains of ZFxHunt (0 - 18 fingers, as indicated). ZFP are not fused to any effector domain. The pTarget vector does not contain ZFP and is used as a control. **(A)** FACS assay measuring the fold-reduction in EGFP or HcRED fluorescent cells, in response to different zinc fingers. A 5-fold repression is equivalent to 80% reduction. **(B)** qRT-PCR assay to measure fold-repression of EGFP or HcRED mRNA by ZFP.**(C)** EGFP Western blot for ZFP repression of pEH-Qx targets. β-actin staining is used as a loading control.

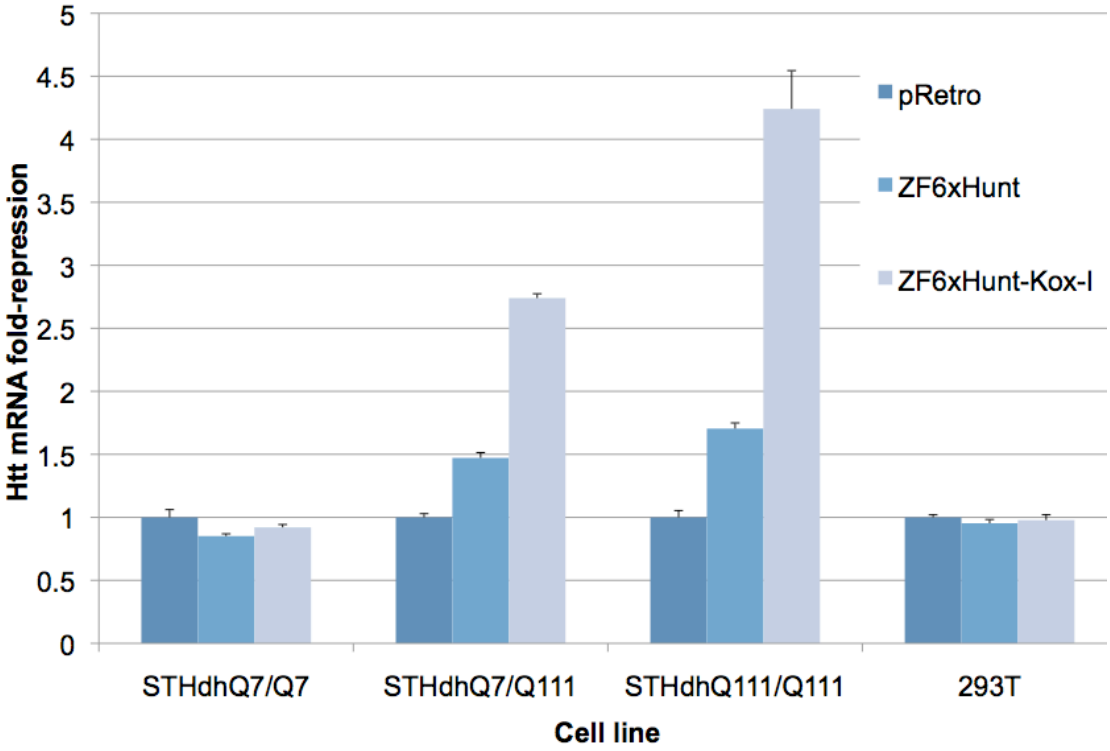

Figure S3. Repression of chromosomal CAG-repeat genes, 20 days after retroviral ZFP delivery, in homozygous and heterozygous cells. Assays were carried out in wt mouse ST*Hdh* cells (Q7/Q7), in homozygous poly-Q ST*Hdh* mutants (Q111/Q111), in heterozygous poly-Q ST*Hdh* mutants (Q7/Q111), and in human HEK293T cells, as indicated. qRT-PCR was used to compare *HTT* mRNA levels (mRNA fold-repression). Mouse primers that do not discriminate between wt or mut *HTT* were used, and consequently, repression of *HTT* in heterozygous STHdh cells was approximately half of that was seen in homozygous mutant STHdh cells, suggesting that the levels of repression seen correspond to repression of mutant *HTT*.

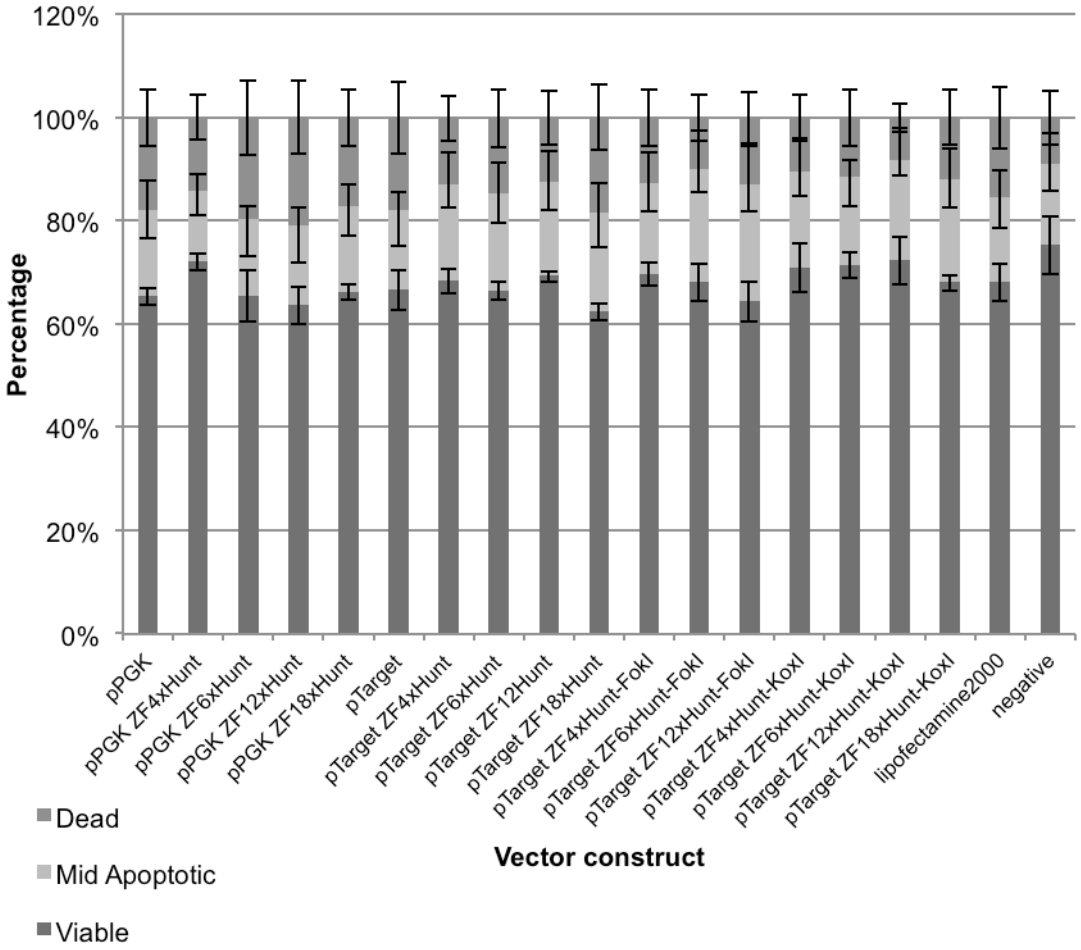

Figure S4. ZFxHunt toxicity assay. HEK-293T cells were transfected with 400 ng of the indicated vector constructs using Lipofectamine2000 and harvested 48 hours after transfection. As a control Lipofectamine2000-only or untransfected cells (negative) were used. Cytotoxicity was analyzed using Guava Cell Toxicity (PCA) Assay according to manufacturer's instructions. Results show the percentage of dead mid-apoptotic and viable cells. Bars express results of at least 3 independent experiments. In conclusion, ZFxHunt proteins do not appear to be toxic.

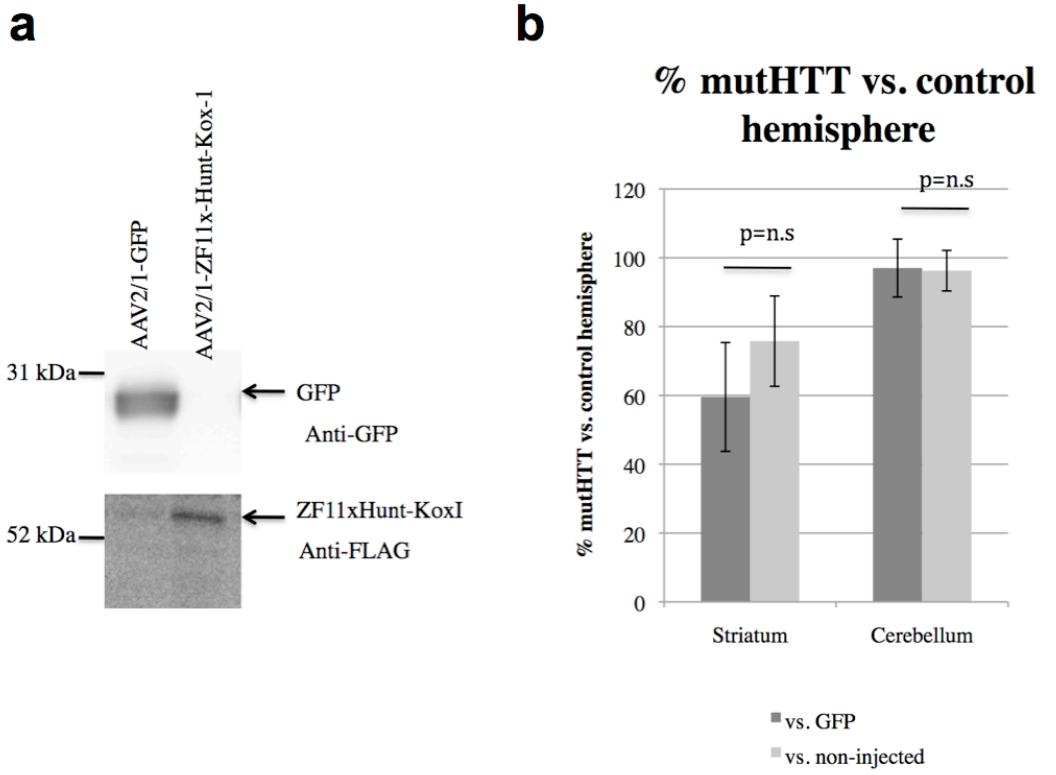

Figure S5. (A) Western blot of dissected striatum shows expression of GFP in one hemisphere and ZF11xHunt-Kox-1 (with FLAG-tag) in the other, corresponding with injections. **(B)** qRT-PCR data quantifying % of mut *HTT* mRNA vs control hemisphere in mouse striatal samples injected with ZF11xHunt-Kox-1 in one hemisphere. The other hemisphere was either injected with GFP, n=3 (dark grey) or non-injected, n=3 (light gray). Cerebellum was non-injected. There are no statistically-significant differences, indicating that the effect observed is due to repression by zinc fingers, and not to a toxic effect by GFP. Student's T-test p-values: 0.18 (striatum) and 0.48 (cerebellum).

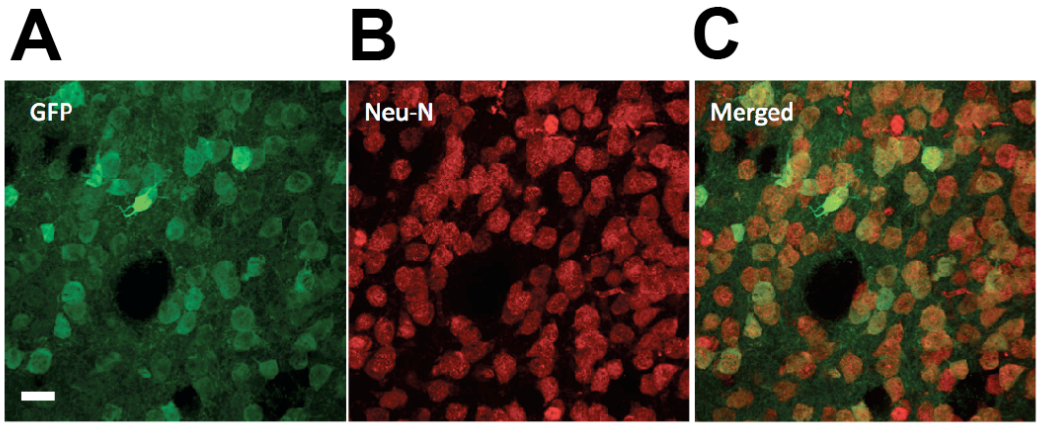

Figure S6. Assaying the cellular targeting of AAV2/1 by immunohistochemistry. (A) GFP fluorescence (green) reveals AAV2/1 transduction in a striatal section (scale bar: 10 μm). (B) Anti-NeuN immunofluorescence (red) marks neuronal cell bodies as previously shown in Ref. 37. (C) The merged image reveals AAV2/1 transduction of neurons, together with NeuN, showing that transgene expression coincides with a neuronal cell marker. It should be noted that while the AAV1 capsid protein does have neuronal tropism, it also efficiently transduces most glial and some ependymal cells.

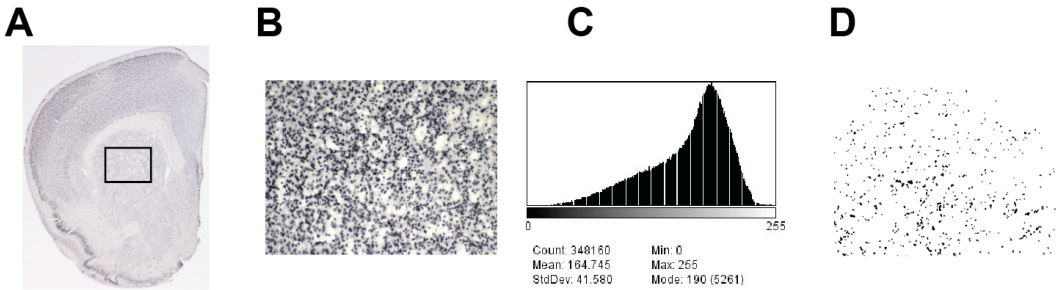

Figure S7. Quantifying HTT-positive aggregates by automatic counting of mut HTT positive particles with ImageJ software, using the method of Moncho-Bogani et al. (*Neurosci* **21**(8):2186-2198). (A) Using mut HTT-immunostained coronal slices, a region of interest of 650 x 865 μm^2, was selected in the middle of the dorsal striatum (10X objective). (B) Background was subtracted and the image was converted to 8-bit. (C) A grey-level histogram was calculated and a threshold of 70% of the mode was used for binarization (i.e, leaving particles showing a grey level >30% of the mode). (D) The image was filtered with an erosion-dilation filter to eliminate noise and the number of remaining particles was automatically counted. Counts were made in 4 serial slices, separated by 240 μm, and averaged providing a single density measure per hemisphere. Counts were then calculated per 0.1 mm^2.

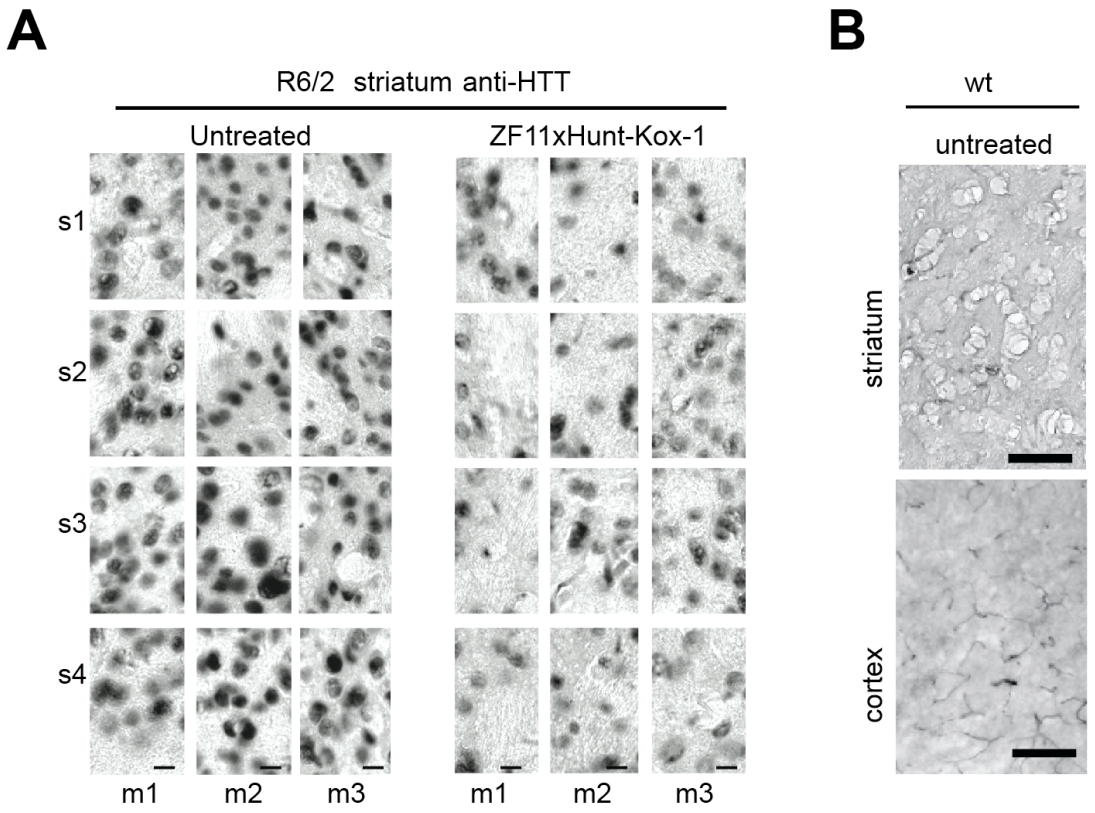

Figure S8. Anti-HTT immunostaining of the striatum and cortex of R6/2 and wt mice. (A) Staining R6/2 striata reveals a reduction of the intensity of mutant aggregates with ZF11xHunt-Kox-1 treatment. Data are from three mice (m1, m2 and m3) and from four brain sections per mouse (s1-s4). The treated and untreated hemispheres are stained simultaneously within each section. Close-ups are shown to aid visualisation (see main Fig. 6C for wide-field views). The automated HTT counting method used wide-field views (Fig. S7). (B) Sections from wild-type (wt) mice are shown for comparison and contain no mut HTT aggregates. Scale bars: 10μm for R6/2; 100 μm for wt.

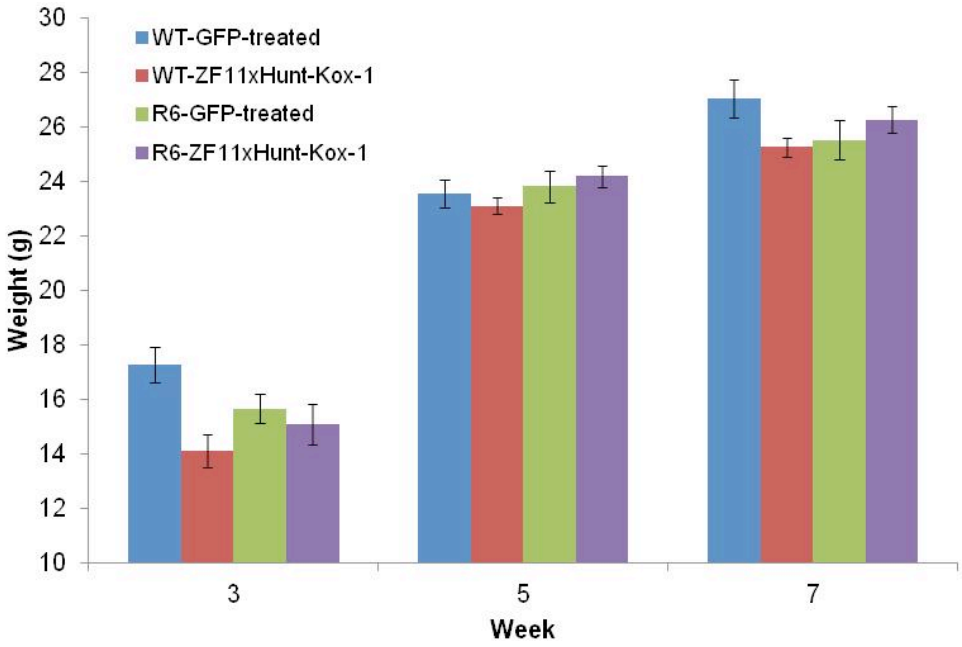

Figure S9. Weight of R6/2 mice and their WT littermate groups across 3 weeks during which the rotarod assay was carried out. An ANOVA of repeated measures with Group as between subject factor and Week as within subject factor revealed a significant main effect of Week ($F_{2, 47}$=435, p<0.001) but not of Group ($F_{3, 47}$=2.41, p=0.079). All measures Mean±S.E.M. WT-GFP-treated (n=14), WT- ZF11xHunt-Kox-1 treated (n=14); R6/2-GFP treated (n=12); R6/2-ZF11xHunt-Kox-1 treated (n=12).